Water Resources Research

RESEARCH ARTICLE
10.1029/2018WR022800

Physical and Chemical Controls on the Simultaneous Occurrence of Young and Old Groundwater Inferred From Multiple Age Tracers

S. C. Underwood[1,2], J. L. McCallum[1,2,3], P. G. Cook[2,3], C. T. Simmons[2,3], S. Dogramaci[2,4], R. Purtschert[5], A. J. Siade[1,2,6], and H. Prommer[1,2,6]

[1]School of Earth Sciences, University of Western Australia, Crawley, Western Australia, Australia, [2]National Centre for Groundwater Research and Training, Flinders University, Adelaide, South Australia, Australia, [3]College of Science and Engineering, Flinders University, Adelaide, South Australia, Australia, [4]Rio Tinto Iron Ore, Perth, Western Australia, Australia, [5]Climate and Environmental Physics, Physics Institute, University of Bern, Bern, Switzerland, [6]CSIRO Land and Water, Floreat, Western Australia, Australia

Key Points:
- Numerical experiments were used to define envelopes of apparent groundwater age discrepancies that can be explained by physical mixing mechanisms (and those that cannot)
- Matrix diffusion represented by a dual-domain mass transfer model can partially explain observed age discrepancies
- Where samples fall outside these physical mixing envelopes, chemical reaction processes affecting ^{14}C activity need to be considered to explain observed age discrepancies at the study site

Supporting Information:
- Supporting Information S1

Correspondence to:
H. Prommer,
henning.prommer@csiro.au

Citation:
Underwood, S. C., McCallum, J. L., Cook, P. G., Simmons, C. T., Dogramaci, S., Purtschert, R., et al. (2018). Physical and chemical controls on the simultaneous occurrence of young and old groundwater inferred from multiple age tracers. *Water Resources Research*, *54*. https://doi.org/10.1029/2018WR022800

Received 16 FEB 2018
Accepted 13 OCT 2018
Accepted article online 24 OCT 2018

Abstract Understanding groundwater ages within an aquifer system has the potential to better constrain estimates of groundwater recharge and flow rates and therefore increase the reliability of groundwater models. Groundwater ages are generally interpreted from field-observed environmental tracer concentrations, but in many cases in which multiple groundwater age tracers have been analyzed simultaneously the results show significant disparities among tracer-specific estimated ages. The disparities are generally attributed to physical mixing between waters of different ages. However, especially in the geochemical literature environmental tracer concentrations are often analyzed with simplistic models in which the degree of the simulated mixing might be considered unrealistic for natural heterogeneous geologic media. In this study we use numerical experiments to examine under which physical conditions measured concentrations of selected environmental tracers (CFC-12, ^{39}Ar, and ^{14}C) may return discrepant ages. Our model simulations suggest that matrix diffusion has the greatest potential to cause mixing of different-aged water and to generate age biases between tracers. The multitracer simulations also suggest that there is a limit to the magnitude of the discrepancies that can be attributed to physical processes. When comparing data collected from the Pilbara region of Western Australia with our numerical modeling studies, it was found that a dual-domain mass transfer model was required to explain the field-observed age discrepancies.

1. Introduction

Understanding and quantifying the distribution of groundwater ages within an aquifer system provides a significant potential to better constrain estimates of groundwater recharge and flow rates (Cook & Robinson, 2002; Solomon et al., 1993; Vogel et al., 1974) and therefore improve the reliability of groundwater flow models (Michael & Voss, 2009; Reilly et al., 1994; Sanford, 2011; Sanford et al., 2004; Turnadge & Smerdon, 2014; Yager et al., 2013). However, the age of groundwater can never be directly measured but must be inferred from measured concentrations of selected individual or multiple environmental tracers such as tritium (^{3}H), chlorofluorocarbons (CFCs), carbon-14 (^{14}C), or argon-39 (^{39}Ar). Where groundwater ages are deduced from measured concentrations of multiple environmental tracers, they often indicate mixtures of waters of different apparent ages (Bethke & Johnson, 2008; Cornaton & Perrochet, 2006; Ginn, 1999; Suckow, 2013; Varni & Carrera, 1998). Concentrations of environmental tracers that are indicative of relatively young waters ($<$60 years) and concentrations of tracers indicative of very old water have been found in the same groundwater samples at a wide range of field sites, as seen in Figure 1 (e.g., Alikhani et al., 2016; Arslan et al., 2015; Bretzler et al., 2011; Cook et al., 2005, 2017; Corcho Alvarado et al., 2007; Genereux et al., 2009; Harrington, 2002; Jasechko et al., 2017; Jurgens et al., 2014, 2016; Massoudieh et al., 2014; Samborska et al., 2013; Sültenfuβ et al., 2010; Talma et al., 2000). Cook et al. (2005), for example, observed the presence of CFCs, an indicator of water less than 60 years old, in water with ^{14}C concentrations suggesting ages of thousands of years in a fractured rock aquifer. Similarly, Genereux et al. (2009) reported CFC concentrations in samples with ^{14}C concentrations implying the sampled water in the Braulio Carrillo National Park, Costa Rica, is older than 8,000 years. Most recently, groundwater samples from bores within the Pilbara region of

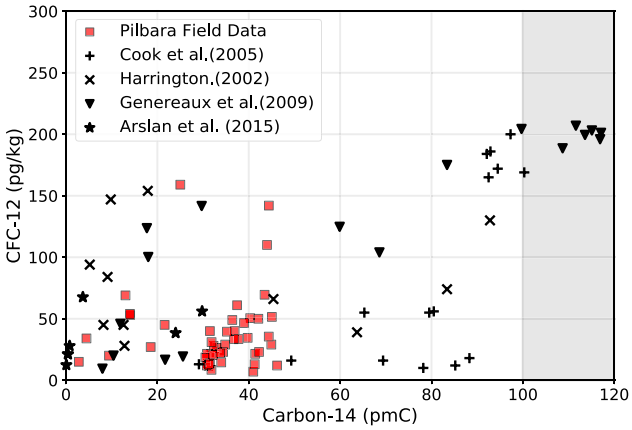

Figure 1. Comparison between CFC-12 concentrations and ^{14}C activities as reported from samples collected at selected at field sites. Any sample with CFC-12 indicates recent recharge, while a ^{14}C concentration $<$100 pmC indicates older water. Modern ^{14}C concentrations are considered to be $>$100 pmC, and also indicate recent recharge.

Western Australia have been found to contain both measurable CFC-12 and uncorrected ^{14}C activities of 30–40 pmC, also suggesting the mixing of old groundwater with recent recharge (Cook et al., 2017; McCallum et al., 2017). Even when accounting for geochemical processes, Jasechko et al. (2017) found ^{3}H in samples with depleted levels of ^{14}C indicating the mixing of young and fossil age groundwater.

Physical mixing of waters of different ages occurs over various time frames during subsurface passage as a result of diffusion, transverse dispersion (Castro & Goblet, 2005), and diffusive mass transfer between permeable zones of an aquifer and poorly permeable layers such as aquitards (Cornaton & Perrochet, 2006; LaBolle et al., 2006; Sanford, 1997; Weissmann et al., 2002). Various sampling conditions, such as long-screened wells, can also induce physical mixing of waters of different age through the interception of multiple flow paths (Hofmann et al., 2010; Małoszewski & Zuber, 1982). Additionally, chemical processes may cause erroneous interpretation of the true groundwater age for one or more of the analyzed tracers. For ^{14}C, these processes include dissolution of old carbonates and fractionation due to reactions including ion exchange and oxidation-reduction (Clark & Fritz, 1997; Salmon et al., 2015). CFCs are also prone to sorption and degradation under specific conditions (Bauer et al., 2001; Cook & Solomon, 1995; Hinsby et al., 2007), which can influence tracer concentrations and create bias in groundwater age dating.

Where samples are thought to represent a mixture of waters of different apparent ages, the interpretation of environmental tracer concentrations is frequently carried out with analytical models (e.g., International Atomic Energy Agency, 2006; Maloszewski & Zuber, 1996). These models quantify the mixtures of young and old groundwater and their relative distributions using mathematical functions. Common tracer interpretation models include lumped parameter models (e.g., Amin & Campana, 1996; Maloszewski & Zuber, 1982, 1996; Zuber, 1986) and direct age models (Ginn, 1999; Goode, 1996). In several studies the groundwater age distributions determined from these models have been employed to assist in the characterization of groundwater dynamics (e.g., Corcho Alvarado et al., 2007; Eberts et al., 2012; Gusyev et al., 2013; Long & Putnam, 2009; Solomon et al., 2010; Troldborg et al., 2007; Zuber et al., 2005).

While mixing models are well developed in the literature, an important shortcoming is that they do not explicitly simulate physical mixing mechanisms and therefore potentially allow for physically unrealistic scenarios. To date, only few studies have sought to employ process-based models to more closely interrogate measured field data of multiple environmental tracers and to investigate how various types of physical transport mechanisms can affect interpreted groundwater ages (Cook et al., 2005; Gardner et al., 2015; McCallum et al., 2014). Therefore, this study systematically explores and discusses the influence of different physical transport processes on generating mixing between young and old groundwater and to what extent they can contribute to field-observed apparent age discrepancies.

We define and perform a range of numerical experiments with a synthetic two-dimensional (2-D) aquifer system to illustrate and quantify the coupled transport and mixing of multiple environmental tracers. For our simulations we employ three representative groundwater age tracers. We use CFCs to denote young groundwater and ^{14}C, which is commonly used to date groundwater from ~2,000 years up to as old as 30,000 years. In addition, we also simulate the transport of the less commonly applied ^{39}Ar, which covers an intermediate age range between the preceding two (50 to 1,000 years). Our simulations do not take into account external processes (e.g., degradation of CFCs or subsurface production of ^{39}Ar) that may influence the concentrations of these tracers within the subsurface. Any samples that can't be explained by physical processes must therefore be produced by such reactions. This allows us to isolate the influence of individual processes on the sampled field data. Transport of environmental tracers is explored in both porous media and fractured rock. For the latter we employ a dual-domain approach in which the mobile domain represents fracture flow and the immobile domain represents the rock matrix. For the larger-scale setting investigated here a dual-domain approach was preferred to represent the transport characteristics of fractured rock aquifers, thereby omitting the need for an explicit parameterization of the fracture network that would have been

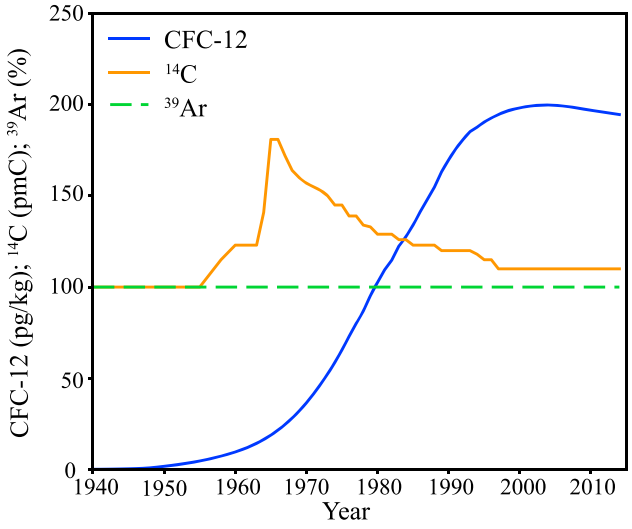

Figure 2. Atmospheric concentrations of environmental tracers as used for simulated groundwater recharge concentrations between 1940 and 2015. CFC-12 data are based on measured atmospheric concentrations at Cape Grimm (Cunnold et al., 1994) and ^{14}C data are based on Levin et al. (1992). ^{39}Ar was set to the globally constant value of 100% modern (Corcho Alvarado et al., 2007).

required when employing a discrete fracture network model. Potential influences on the observed tracer concentrations such as (i) sampling conditions, (ii) recharge variability, and (iii) previously unaccounted geochemical reactions are also investigated.

In light of these theoretical model simulations, we analyze the recently reported field measurements of environmental tracer concentrations obtained from a site within the Pilbara region of northwestern Australia (Cook et al., 2017; McCallum et al., 2017). We use the environmental tracer distributions produced from the model simulations to identify which physical processes could plausibly explain the observed apparent age discrepancies in the field data.

2. Methodology

2.1. Considered Environmental Tracers

The transport of three commonly used environmental tracers that span a broad range of temporal scales was considered for this study; CFC-12, ^{39}Ar, and ^{14}C. Carbon-14, a naturally occurring isotope with a half life of 5,730 years, can be used to date groundwater from ~2,000 up to around 30,000 years old and is one of the most widely used tracers in groundwater studies (Clark & Fritz, 1997). Groundwater apparent age determination with ^{14}C relies on the well-defined radioactive decay from an initial ^{14}C activity at the time groundwater is recharged, which is usually assumed to be 100 pmC (Kalin, 2000). However, in natural systems, rock-water interactions can have a large influence on ^{14}C (Clark & Fritz, 1997; Salmon et al., 2015). A number of correction techniques that account for the sample's $\delta^{13}C$ signature allow corrections to be made for ^{14}C activities resulting from chemical reactions (Han & Plummer, 2013; Ingerson & Pearson, 1964; Mook et al., 1974).

Chlorofluorocarbon-12 (CFC-12) atmospheric concentrations have rapidly increased since the 1940s as a result of industrial and domestic uses, peaking in the 1990s (see Figure 2). Accordingly, the presence of CFCs in groundwater indicates recharge post-1940 (Busenberg & Plummer, 1992). Since the atmospheric accumulation of CFCs has been well documented, in theory, the year of recharge and hence groundwater age can be determined from CFCs by relating the measured concentrations in groundwater back to the known historical atmospheric concentrations (International Atomic Energy Agency, 2006). It should be noted, however, that sorption and degradation processes under anaerobic conditions have the potential to bias dating with CFCs (most notably CFC-11) (Bauer et al., 2001; Cook & Solomon, 1995; Hinsby et al., 2007). Due to the declining trend in atmospheric CFC concentrations since the 1990s, age dating with CFC's after this time may not give a unique solution.

Argon-39, with a half life of 269 years can be used to date groundwater in the range of 50 to 1,000 years (Loosli et al., 2000), making it a useful tracer to cover the intermediate timescales between the young age tracers (CFCs) and ^{14}C. As ^{39}Ar has a constant and well-known atmospheric input concentration and is unaffected by anthropogenic sources; age dating is achieved by assuming that the reduction in the concentration of groundwater is solely due to radioactive decay.

2.2. Pilbara Field Site

The considered field site is located approximately 80 km northwest of Newman in Western Australia within the Hamersley Basin. The region has a highly variable arid to semiarid climate, with rainfall being primarily associated with tropical cyclones over the summer months. The target aquifers at the site are the fractured Marra Mamba Banded Iron Formation overlain by the Wittenoom formation, which is composed of shale, dolomite, and sandstone and is considered to be the main regional aquifer. Further details of the Pilbara field site can be found in Cook et al. (2017) and Dogramaci et al. (2012). A total of 48 water samples were taken from production bores in 2008, 2014, and 2016 and analyzed for CFC-12 and ^{14}C. The samples collected in 2008 and 2014 are reported in Cook et al. (2017). Nine ^{39}Ar samples were collected as reported in McCallum et al. (2017). In addition, this study includes newly analyzed ^{14}C and CFC-12 data collected in

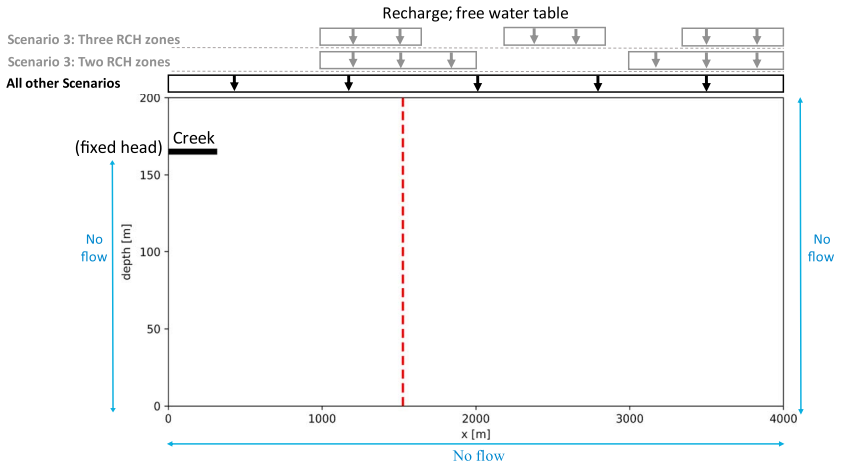

Figure 3. Schematic of the 2-D simulation domain, including dimensions and boundary conditions. The vertical dashed red line shows the location of the monitoring wells. Recharge is considered to be spatially uniform except in Scenario 3, where recharge is nonuniformly distributed.

2014 and 2016 from additional bores. The sampled bores ranged in depth from 120 to 216 m and were completed with 300-mm steel casing. The screened intervals ranged from 12 to 158 m in length. Most of the sampled bores were continuously pumped for dewatering. However, bores that were not being pumped were purged a minimum of three bore values, and sampling was only carried out when field measurements of electrical conductivity, temperature, and pH had stabilized. The sampling techniques used to obtain these environmental tracer samples are detailed in Cook et al. (2017) and are therefore only briefly described here. Samples for ^{14}C and ^{13}C were collected in 500-ml plastic bottles, and analysis was carried out at GNS Science Rafter Radiocarbon Laboratory using accelerator mass spectrometry and isotope ratio mass spectrometry, respectively. Groundwater samples for CFCs were collected in 125-ml glass bottles submerged in a bucket with several volumes flushed prior to sampling to avoid atmospheric contamination. CFC concentrations were determined at the GNS Science Water Dating Laboratory by gas chromatography. In addition, ^{39}Ar concentrations reported in McCallum et al. (2017) were obtained from gas samples taken in situ. Gas samples of 6.5 bar in 6-kg cylinders were obtained by degassing between 3.3 and 4.3 m^3 of water in the field (Purtschert et al., 2013). The samples were analyzed at the University of Bern, Switzerland, using low level gas proportional counting (Loosli et al., 1986; Loosli & Purtschert, 2005; Riedmann & Purtschert, 2016).

2.3. Numerical Modeling Framework

2.3.1. Numerical Model Setup

A quasi-hypothetical, synthetic, relatively simple 2-D cross-sectional model was defined to perform the numerical experiments (Figure 3). The selected model setup represents an unconfined aquifer, 4-km long and 200-m deep, loosely based on aquifer geometries observed at the Pilbara site by Cook et al. (2017). A 2-D model geometry was selected over a full 3-D model for the sake of higher computational efficiency while not significantly compromising the general findings as per previous studies (D'Affonseca et al., 2011; Ekwurzel et al., 1994; Ma et al., 2014; Salmon et al., 2015; Solomon & Sudicky, 1991; Zhang et al., 2013). Groundwater flow was simulated with MODFLOW-NWT (Niswonger et al., 2011) and multispecies environmental tracer transport simulations were performed with MT3DMS-USGS (v1; Bedekar et al., 2016).

The conceptual hydrogeological model was defined to resemble a semiarid groundwater system. In the selected setup, all water enters the domain through groundwater recharge and exits the domain through a creek situated on the left boundary of the domain represented through a specified head boundary condition. No flow was permitted across the lateral and bottom boundaries, which represent the groundwater divide in the recharge area and an underlying impermeable layer, respectively (Figure 3). The hydraulic properties of the aquifer (Table 1) were chosen to be representative of a limestone/dolomite aquifer (Freeze & Cherry, 1979).

Table 1
Model Parameters Used in Simulations

Parameter	Unit	Value
Domain length (x direction)	m	4,000
Domain depth (z direction)	m	200
Horizontal discretization (x direction)	m	50
Vertical discretization (z direction)	m	2
Hydraulic conductivity	m/day	0.1
Hydraulic conductivity anisotropy ratio	—	0.1
Effective porosity (θ)	—	0.2[a]
Specific storage	m^{-1}	1×10^{-6}
Specific Yield	—	0.2
Longitudinal dispersivity (α_L)	m	10[b]
Recharge Rate	mm/year	5[c]

[a]Freeze and Cherry (1979). [b]Gelhar, Welty, Rehfeldt, et al. (1992). [c]Chloride mass balance presented in Cook et al. (2017).

2.3.2. Simulation of Environmental Tracer Concentrations

Reconstructed atmospheric concentration histories for individual tracers were aggregated to annual averages and assigned as recharge concentrations (Figure 2). In this study, southern hemisphere concentrations were adopted for CFCs and ^{14}C, as reported by Cook et al. (2017). CFC recharge concentrations are based on measured atmospheric concentrations at Cape Grimm (Cunnold et al., 1994), converted to equivalent aqueous concentrations based on the solubilities of the respective gases (Warner & Weiss, 1985). A recharge elevation of 600 m, a recharge temperature of 24 °C, and negligible amounts of excess air were assumed. The ^{14}C activities in atmospheric CO_2 were adopted from Levin et al. (1992), and the atmospheric input for ^{39}Ar was set to the globally constant value, that is, 100% modern (Corcho Alvarado et al., 2007). First-order decay of environmental tracers was modeled, where applicable, using the decay rate constants listed in Table 2. Species-specific molecular diffusion coefficients as employed in the simulations are also listed in Table 2.

The transport simulations were performed in two steps. In the first step the spatial distributions of ^{14}C and ^{39}Ar concentrations were obtained by computing the steady state transport solution (Zheng, 2010) under the implicit assumption of a steady state flow field. This step assumed a recharge concentration of 100 pmC and 100 pmA, for ^{14}C and ^{39}Ar, respectively, which are considered the long-term natural background concentrations (Corcho Alvarado et al., 2007; Kalin, 2000). In the second step the computed steady state concentrations were used to define the initial concentrations of ^{14}C and ^{39}Ar for a subsequent 75-year long transient transport simulation. This simulation started in 1940 and considered the temporally variable concentration input that occurred for CFC-12 during this period (Figure 2) as well as for ^{14}C, which exceeded 100 pmC from the 1950s as a result of nuclear weapon testing (Cook & Böhlke, 2000). Note that the steady state transport solution requires a fraction of the runtime needed by an equivalent transient transport model for a sufficiently long period (up to 30 kyr) until a steady state is reached.

2.3.3. Long-Screen Monitoring Wells

Where samples are collected from short-screened monitoring wells, the origin of the sampled groundwater with respect to the sampled depth is well defined as the mixing of waters from different depths and therefore different ages are insignificant. In contrast, groundwater samples obtained from long-screened wells represent mixtures of waters from different depths and, depending on the geology, potentially vastly different flow paths, leading to water mixtures of highly disparate ages (Eberts et al., 2012; Visser et al., 2013; Zinn & Konikow, 2007b). To quantify this effect, we consider tracer concentrations as determined from a range of screen lengths for each of the investigated scenarios and accordingly determine the respective influence on mixing and apparent age discrepancies. Monitoring wells of screen lengths spanning 10, 20, 40, 80, 100, 120, 140, and 160 m at all depths within the domain are considered by successively moving the wells within the domain along a vertical line, that is, positions indicated by the red line in Figure 3. For each well position, the flux weighted average concentration was extracted from the mobile domain of the aquifer. As the hydraulic gradient within the domain in primarily horizontal, there is minimal variation in tracer concentrations laterally across the domain (Vogel, 1967), so only vertical locations were systematically altered. An exception to this was made when the recharge was varied spatially across the domain, with the lateral locations chosen such that they would be in a position which yields maximum discrepancy.

Table 2
Decay Constants and Diffusion Coefficients of Tracers Studied

Tracer	Half life (years)	Radioactive decay constants ($year^{-1}$)	Free solution diffusion coefficient (m^2/year)
CFC-12	—	—	3.5×10^{-2}
^{14}C	5,730	1.21×10^{-4}	4.0×10^{-2}
^{39}Ar	269	2.58×10^{-3}	2.68×10^{-2a}

Note. Data from Cook and Herczeg (2000) except where specified.
[a]Maharajh and Walkley (1973).

2.4. Numerical Experiments

Systematic numerical simulations were conducted to assess the effectiveness of different physical mechanisms in reproducing field-scale groundwater age discrepancies. Starting with the classical Fickian dispersion model, we investigated the effectiveness of individual processes and of plausible combinations of processes.

Table 3
Parameters of Fickian Advection-dispersion Model

Parameter	Unit	Range considered
Longitudinal dispersivity (α) (α_L)	m	0–140
Transverse dispersivity (α_T)	m	$0.1 \times \alpha_L$
Effective Porosity	—	0.2
Recharge Rate	mm/year	5

2.4.1. Scenario 1: Advection-Dispersion With Fickian Macrodispersion (Homogeneous)

In a first step, we investigated the maximum possible apparent age discrepancies that may be produced under a Fickian advection-macrodispersion model (ADM). Note that previous studies have pointed out that the ADM is mostly appropriate to describe tracer transport in relatively homogeneous porous media (Ekwurzel et al., 1994) and its accuracy decreases as aquifer heterogeneity increases (Feehley et al., 2000; Larocque et al., 2009). The ADM implies that solute spreading is fundamentally diffusive in nature with the magnitude of the velocity-dependent dispersion phenomena being controlled by the longitudinal dispersivity (α_L; L) and the transverse dispersivity (α_T; L), which has a horizontal (α_{TH}; L) and vertical (α_{TV}; L) component in two dimensions. The ranges of the investigated values are shown in Table 3. Employed molecular diffusion coefficients differed between environmental tracer species but remained constant throughout all simulations in accordance with Table 2.

2.4.2. Scenario 2: Dual-Domain Mass Transfer (DDMT)

In highly heterogeneous environments dual-domain mass transfer models have often been shown to provide a more suitable alternative to the standard advection-dispersion formulation (Feehley et al., 2000; Harvey & Gorelick, 2000; Julian et al., 2001; Liu et al., 2007). Dual-domain models have also been successfully applied for solute transport simulations in fractured rock aquifers (e.g., Gusyev et al., 2013). Solute transport in fractured rocks is characterized by rapid advective transport through the fractures, with slow diffusive exchange between water moving through the fractures and the effectively stagnant water within the rock matrix (Maloszewski & Zuber, 1991; Małoszewski & Zuber, 1985; Neretnieks, 1980; Sudicky & Frind, 1982). Previous studies have found that diffusion of ^{14}C into the matrix can significantly affect the interpreted apparent groundwater ages (Maloszewski & Zuber, 1991; Neretnieks, 1981; Sanford, 1997; Sudicky & Frind, 1981) and several studies have attributed significant discrepancies between apparent ages interpreted from multiple tracers to matrix diffusion (Cook et al., 2005; Cook & Robinson, 2002; LaBolle et al., 2006; Neumann et al., 2008; Sanford et al., 2017). The majority of these studies investigated discrete fracture networks at a relatively small scale, while only two of the studies have adopted the dual-domain modeling approach. Among those, Neumann et al. (2008) illustrated the influence of mass transfer processes on ^{3}H-^{3}He age dating, and more recently, Sanford et al. (2017) simulated young age tracers (^{3}H, CFCs, and SF_6) along flow paths to partially constrain dual-domain parameters.

The main parameters controlling a dual-domain system are the mobile (θ_m) and immobile porosity (θ_{im}) and the mass transfer coefficient (β), which controls the rate of solute exchange between mobile and immobile zones (Zheng & Wang, 1999). In our DDMT scenarios both the ratio of immobile to mobile domain porosities and mass transfer rates were varied (Table 4) to explore the effects of matrix diffusion, over a wide spectrum of possible dual-domain parameter values, on the general pattern of tracer distributions and apparent age discrepancies. The mass transfer rate is defined as $\beta = D_e/(\mu l^2)$, where D_e is the effective diffusion coefficient, l is the length over which exchange is occurring, and μ is a shape factor (Sardin et al., 1991). β can also be thought of as the inverse of the mean residence time in the immobile zone; hence, a lower value of β indicates more rapid exchange resulting in conditions representing equilibrium between the mobile and immobile zones being reached over a shorter time. A wide range of values was selected to represent the possible scenarios that may impact on environmental tracer concentrations.

Table 4
Parameters Used in the Dual-domain Scenarios

Simulation	Mobile porosity θ_m	Immobile porosity θ_{im}	Total porosity	Porosity ratio	Mass transfer rate β (year^{-1})	Recharge (mm/year)
1	0.001	0.199	0.2	0.005	$3.65–3.65 \times 10^{-7}$	5
2	0.01	0.19	0.2	0.05	$3.65–3.65 \times 10^{-7}$	5
3	0.02	0.18	0.2	0.1	$3.65–3.65 \times 10^{-7}$	5
4	0.05	0.15	0.2	0.25	$3.65–3.65 \times 10^{-7}$	5
5	0.1	0.1	0.2	0.5	$3.65–3.65 \times 10^{-7}$	5

Table 5
Parameters Used for Spatial Variable Recharge Simulations

Simulation	Porosity (θ)	Mass transfer rate β (year^{-1})	Number of recharge zones	Equivalent recharge (mm/year)
1	0.2	—	2	5
2	0.2	—	3	5
3	0.01; 0.19	$3.65–3.65 \times 10^{-7}$	2	5
4	0.01; 0.19	$3.65–3.65 \times 10^{-7}$	3	5

Note. The range of these parameters is based on the papers discussed (Feehley et al., 2000; Gusyev et al., 2013; Haggerty & Gorelick, 1995; Liu et al., 2007).

2.4.3. Scenario 3: Spatially Variable Recharge

A spatially uniform recharge distribution is the basic assumption of several age dating methods (Cook & Böhlke, 2000) and also a commonly made assumption in numerical modeling studies (e.g., Salmon et al., 2015; Stauffer et al., 2002; Weissmann et al., 2002). However, in most aquifer settings, recharge varies spatially across a catchment due to variations in soil and vegetation cover (Cook et al., 1998), topographic relief (McGuire et al., 2005), localized recharge sources such as surface waters, wetlands or mountain front (Fulton et al., 2012; Siade et al., 2015; Wilson & Guan, 2004), and the variability of vadose zone processes (Scanlon et al., 2002; Wood et al., 2015, 2017). This can result in adjacent groundwater flow paths of very different residence times, which could be expected to create substantial mixing of tracer concentrations indicating distinctively different ages where these flow paths converge, such as in long-screen wells (Wang et al., 2016). To consider how these recharge processes could influence the spatial evolution and interpretation of environmental tracer concentrations, we present a scenario where recharge is distributed over the domain via multiple distinct recharge zones. We considered a case where recharge is applied over two zones each 1,000 m in length, and where recharge is distributed over three zones of 500 m as shown in Figure 3. Equivalent recharge rates were selected such that the same volume of recharge was applied in both scenarios. The parameters used for these simulations are listed in Table 5.

2.4.4. Scenario 4: Temporally Variable Recharge

Temporal variations in groundwater recharge processes are considered a distinctive hydrological characteristic in semiarid regions (Scanlon et al., 2006). Recharge is often highly intermittent, occurring only during high intensity events (Dogramaci et al., 2012). Most modeling studies incorporating environmental tracers are generally based on the assumption of steady state groundwater flow, which includes the assumption of a temporally constant recharge (e.g., Castro et al., 1998; Gassiat et al., 2013; Leray et al., 2016). In reality, however, groundwater ages and environmental tracer concentrations will only be consistent with recharge events or wet periods (McCallum et al., 2017; Schwartz et al., 2010). Therefore, depending on the frequency of recharge events, temporal variability may produce a mechanism which explains the presence of young and old water. Previous studies have suggested that accounting for historic transients (up to 30 kyr) in recharge in the flow system can create a significant difference in apparent age distributions compared to ages simulated using a steady state flow system (Petersen et al., 2014; Sanford et al., 2004; Schwartz et al., 2010).

In the case of the Pilbara region, a number of historic wet and dry climate periods have been identified over the past 2 kyr (Rouillard et al., 2016). Using this information, we compared how transient flow conditions may or may not impact the present day environmental tracer concentration patterns. The recharge during four identified climate periods was approximated while keeping the cumulative sum of recharge equivalent to the steady state rate employed in all previous scenarios (Figure 4). As the exact duration of Period 4 (the mega drought) is unknown, the sensitivity of the present day concentrations to its length is tested with durations of 1 and 10 kyr in alternating simulations. Conditions before this drought period were approximated using a steady state flow and transport simulation assuming infiltration rates equivalent to present-day conditions. Temporally variable recharge was performed in the DDMT model scenario assuming $\theta_m = 0.01$ and $\theta_{im} = 0.19$.

2.5. Quantification of Age Discrepancies

Mixtures were characterized using tracer-tracer concentration plots for all computed flux weighted concentrations from the monitoring wells. These plots were used to determine the sensitivity of these concentration

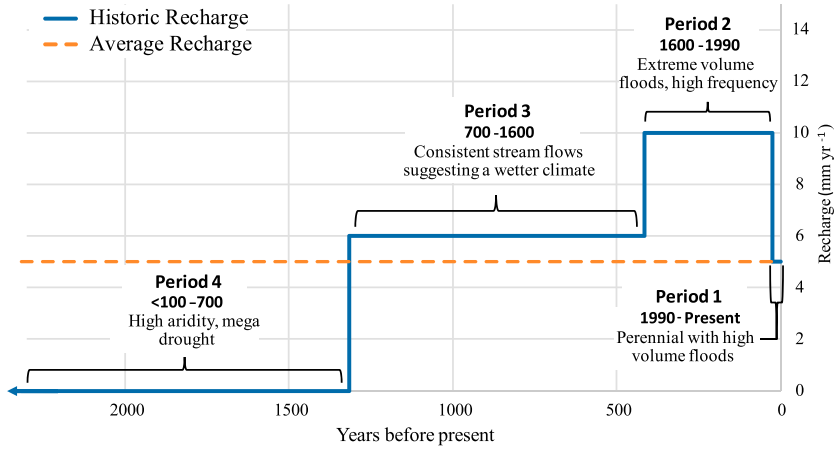

Figure 4. Four identified climate periods in the Pilbara were represented in the model as discrete periods of altered recharge. As the exact length of Period 4 (the mega drought period) is unknown, the length of this period was altered between 1 and 10 kyr.

distributions to the various simulated processes that were investigated in our model scenarios. A sample was considered to be *young* if it contained a concentration of CFC-12 above the analytical detection limit (5 pg/kg), an indicator that the water was recharged post 1950. Samples were considered *old* if they contained ^{14}C activities less than 100 pmC (assuming no analytical errors), which signifies the water was recharged prior to nuclear testing in 1950. As CFC-12 and ^{14}C cannot realistically produce the same apparent age, that is, CFC can only detect young water and ^{14}C is only sensitive to relatively old water, a discrepancy occurs when there are concentrations indicating the presence of CFCs and pre-modern ^{14}C ($<$100 pmC) simultaneously. We refer to this as an *apparent age discrepancy*. All results depict concentrations, as they would have been measured in 2015, based on the assumed input concentrations in Figure 2.

Figures 5f and 6f depict the relationship between tracer concentrations and apparent age discrepancies. The solid lines in these figures depict the *piston flow* line of the tracers for rainfall samples in equilibrium with atmospheric gas concentrations between 1940 and 2015 (Cook et al., 2017). The shaded region on these figures indicates the concentrations that have the potential to arise due to mixing of water.

3. Results and Discussion

3.1. Synthetic Simulation Results

3.1.1. Scenario 1: Advection-Dispersion With Fickian Macrodispersion

For the classic ADM-based scenario (Figures 5a and 6a) very few samples recorded tracer concentrations that were simultaneously indicative of young and old water (i.e., detectable CFC concentrations in waters with ^{14}C activities less than 100 pmC). Figure 5a shows no samples contain CFC-12 concentrations above 20 pg/kg suggesting that only a small amount of CFC's are recharged under the assumed semiarid conditions and these concentrations are further diluted by the long-screen wells. The results showed limited differences between realizations of varying Fickian dispersion parameters suggesting that the results are not highly sensitive to both transverse and longitudinal dispersion (refer to Figures S1 and S2 in the supporting information). Overall results for the ADM closely resemble those that would be obtained with a piston flow model, where all samples would plot exactly on the solid lines or along the *x* axis. This is because the concentration of tracers representing shorter timescales, such as CFC-12, would decrease to zero before ^{14}C concentrations begin to show any noticeable decay. The upper limit of the dispersivity parameters (α_L, α_T) were selected to be within the range of field-scale dispersivities for the appropriate scale aquifer as reported by Gelhar, Welty, Rehfeldt, et al. (1992).

3.1.2. Scenario 2: DDMT

In comparison to the ADM, the results obtained with the DDMT model show a much greater portion of samples with discrepant ages, demonstrating that matrix diffusion can have a notable influence. Figures 5b and 6b present the tracer biases for different length and vertical positions of monitoring wells

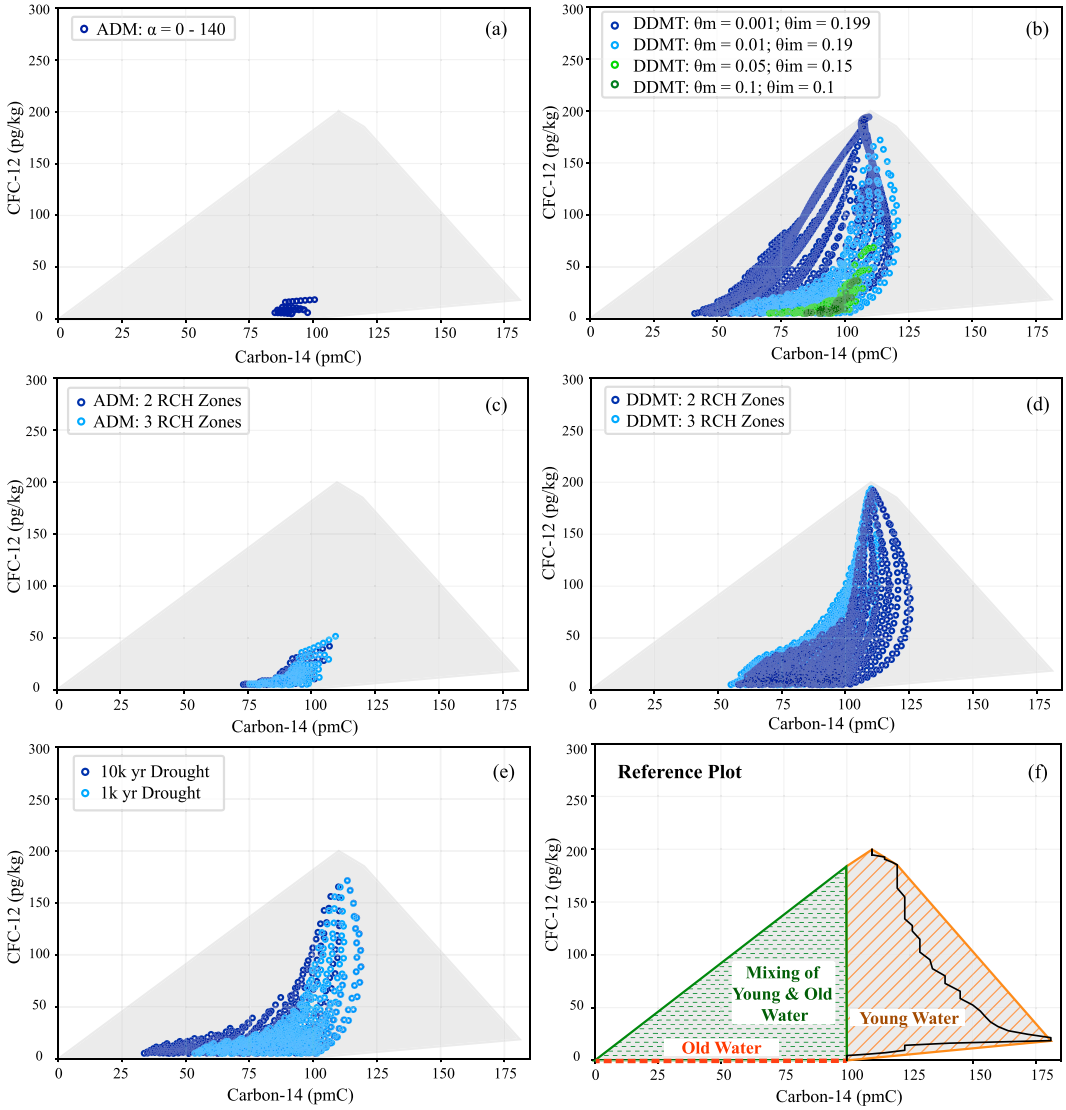

Figure 5. CFC-12 concentrations versus ^{14}C activities. Dots represent iterations of all well screen lengths at all depths throughout the model domain located at x = 1,750 m for each model scenario: (a) Scenario 1 for varying dispersivities, (b) Scenario 2 for varying mass-transfer rates, (c) Scenario 3 using an ADM (θ = 0.2), (d) Scenario 3 using a DDMT model with θ_m = 0.01 and θ_{im} = 0.19, (e) Scenario 4 when altering the duration of the drought period using a DDMT model with θ_m = 0.01 and θ_{im} = 0.19. (f) A reference as to what is considered a mixture of young and old groundwater. The solid lines depict the relationship between concentrations of the tracers for rainfall samples in equilibrium with atmospheric gas concentrations between 1940 and 2015. The shaded regions indicate concentrations that could arise due to mixing of water of different ages. CFC-12 concentrations below the analytic detection limit (<5 pg/kg) have been omitted from the figure. Any point where $^{14}C > 100$ and CFC > 5 pg/kg is considered all young water and would be considered to have no discrepancy. Any point within the green triangle where CFC > 5 pg/kg and $^{14}C < 100$ shows some mixture of young and old groundwater.

for all trialed mass transfer rates. It appears from these figures that the effect of DDMT is more significant for ^{39}Ar data than for ^{14}C. The reason for this is that environmental tracers with shorter half lives are more sensitive to the mixing effect than tracers with longer half lives (McCallum et al., 2014; Varni & Carrera, 1998). Hence, due to the shorter half life of ^{39}Ar, this tracer becomes more sensitive to the mixing of groundwater ages that is induced by the effect of DDMT.

The influence of individual mass transfer rates on recorded concentrations can be found in Figures S3 and S4 in the supporting information. For mass transfer time scales on the order of centuries to millennia (i.e., $\beta = 9.13 \times 10^{-4}$ year^{-1} to 9.13×10^{-5} year^{-1}), matrix diffusion between the two domains causes low ^{14}C activities to be recorded in conjunction with detectable CFC-12. In such cases, diffusion of low concentrations of ^{14}C stored within the immobile matrix back out into the fracture mobile zone enables both young and old

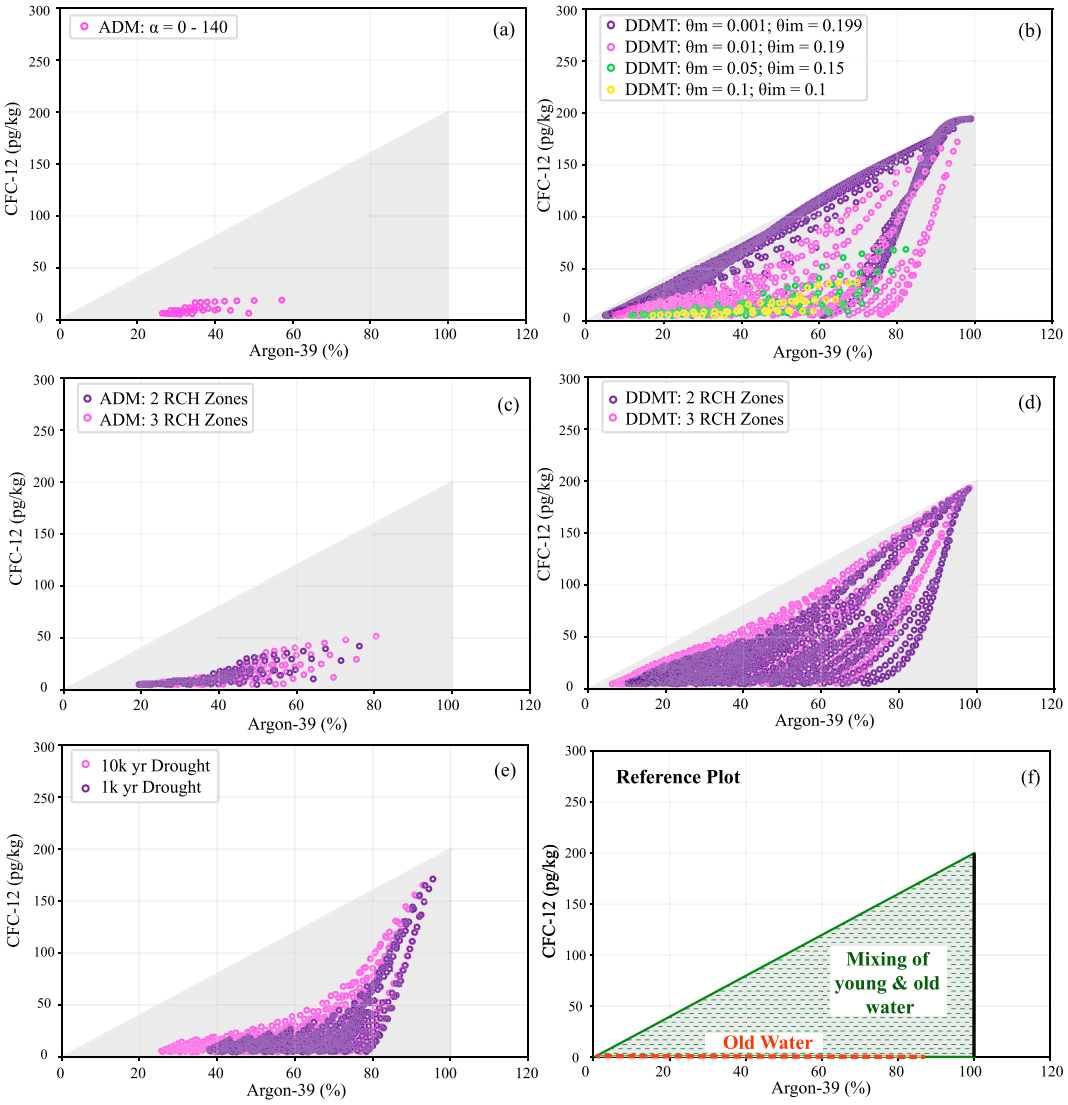

Figure 6. Comparison of the model concentrations of CFC-12 and Argon-39 from all well screen iterations located at x = 1,750 m for each model scenario: (a) Scenario 1 for varying dispersivities, (b) Scenario 2 for varying mass-transfer rates, (c) Scenario 3 using an ADM (θ = 0.2), (d) Scenario 3 using a DDMT model with θ_m = 0.01 and θ_{im} = 0.19, (e) Scenario 4 when altering the duration of the drought period using a DDMT model with θ_m = 0.01 and θ_{im} = 0.19. (f) A reference as to what is considered a mixture of young and old groundwater. The solid lines depict the relationship between concentrations of the tracers for rainfall samples in equilibrium with atmospheric gas concentrations between 1940 and 2015. The shaded regions indicate concentrations that could arise due to mixing of water of different ages. CFC-12 concentrations below the analytic detection limit (<5 pg/kg) have been omitted from the figure any point within the green triangle where chlorofluorocarbons > 5 pg/kg shows some mixing between young and old groundwater.

groundwater to be detected. Below or above this range of rate constants, the effect of DDMT in causing apparent age discrepancies between tracers was not significant. For very low values of β ($<3.65 \times 10^{-6}$ year^{-1}), minimal solute is exchanged into the immobile matrix, therefore causing the models to behave similar to the classic ADM. On the other hand, for high β values ($>3.65 \times 10^{-3}$ year^{-1}) mass transfer occurs so rapidly that the mobile and immobile domain become effectively fully mixed and therefore again behave similar to a single domain ADM.

The larger influence on concentration distributions and age discrepancies caused by matrix diffusion supports the earlier findings of LaBolle et al. (2006). With decreasing mobile porosity (θ_m = 0.001), even lower concentrations of ^{14}C are obtained simultaneously with detectable concentrations of CFCs, as can be seen in Figure 5b. At the same time, ^{39}Ar concentrations show a much narrower range of simulated concentrations, particularly when the mass transfer rate is lower than 9.13×10^{-4} year^{-1}. As the groundwater velocity is

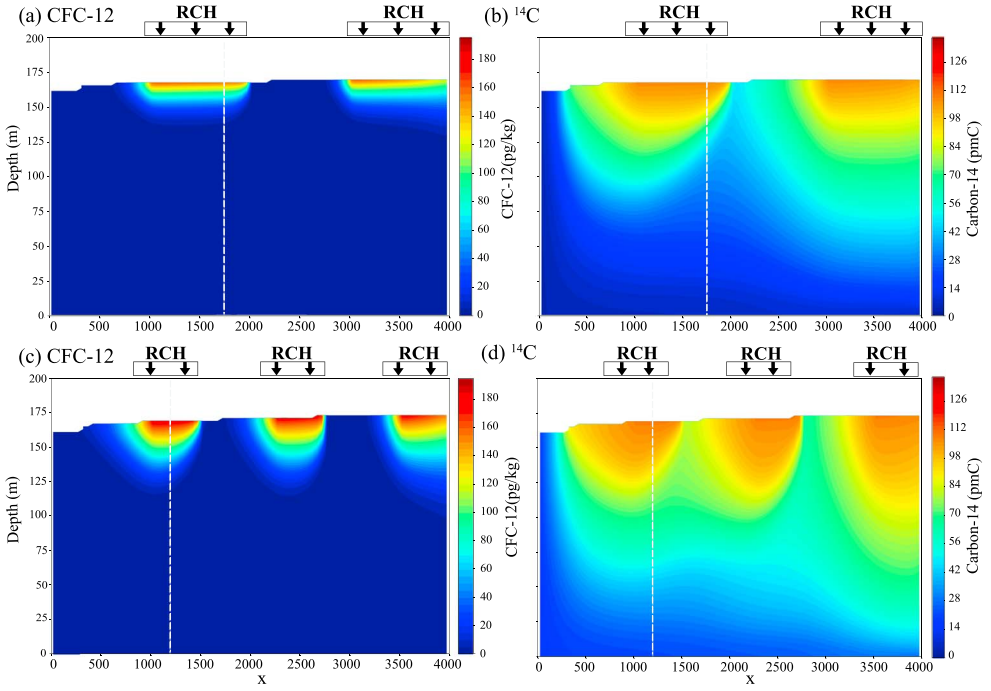

Figure 7. Mobile zone concentrations distributions of CFC-12 and ^{14}C after 75 years for model simulations with two and three distinct recharge zones. The white dashed line indicates the locations of the simulated monitoring boreholes. These monitoring boreholes were positioned to generate the greatest possible discrepancy between tracers. θ_m = 0.01, θ_{im} = 0.19, and $\beta = 3.65 \times 10^{-6}$ year^{-1}.

inversely proportional to the selected value of the mobile porosity, small mobile porosities cause young water to migrate rapidly through the well-connected zones of the system, while older water slowly diffuses out of the immobile matrix. Such a model configuration is representative of a highly fractured system. In simulations with an increased porosity ratio (i.e., when θ_m = 0.1; θ_{im} = 0.1) the model might be more representative of a system containing stratified high-K and low-K layers, as presented in LaBolle et al. (2006) and again later by Neumann et al. (2008). Tracer biases in these simulations returned very similar discrepancies to those obtained with the ADM.

3.1.3. Scenario 3: Spatial Variable Recharge

An illustrative example of the concentration distributions of ^{14}C and CFC-12 created by either two or three distinct recharge zones is shown in Figure 7. Figures 5c and 6c presents the comparison of age biases for these scenarios with CFC-12 concentrations against ^{14}C and ^{39}Ar, respectively. The recharge flux density for the scenario with three recharge zones is 33% higher than the scenario with two recharge zones, which causes younger water to infiltrate to greater depths within the aquifer in the three-recharge-zone scenario as shown in Figure 7. For the ADM setup, incorporating discrete zones of recharge caused a greater number of wells to record discrepancies as detectable amounts of young tracers are now influencing more monitoring screens. These findings support the argument presented in Cook et al. (2017), which suggests that the presence of above-background concentrations of CFC's at significant depths observed in the Pilbara is possibly due to higher vertical flow velocities in areas of localized recharge.

In comparison, recharge variability in the DDMT model does not significantly influence the spread of simulated concentrations (Figures 5d and 6d). This suggests that the influence of the dual-domain behavior itself is much more significant in creating tracer biases within mixtures than the contribution caused by spatially variable recharge. For the DDMT variable recharge scenario, ^{14}C concentrations in all tested monitoring well configurations were lower, particularly for mass transfer rates between 3.65×10^{-4} year^{-1}and 3.65×10^{-5} year^{-1} (Figure S5). A similar effect was also observed for the ^{39}Ar data, but only for mass transfer rates $<9.13 \times 10^{-5}$ yr^{-1} (Figure S6), while otherwise the effect on the ^{39}Ar was minimal. This could be attributed to what Toth (1963) describes as stagnant zones of groundwater that form at the intersection of local, intermediate and regional flow systems. For this study, the vertical line of the monitoring wells was

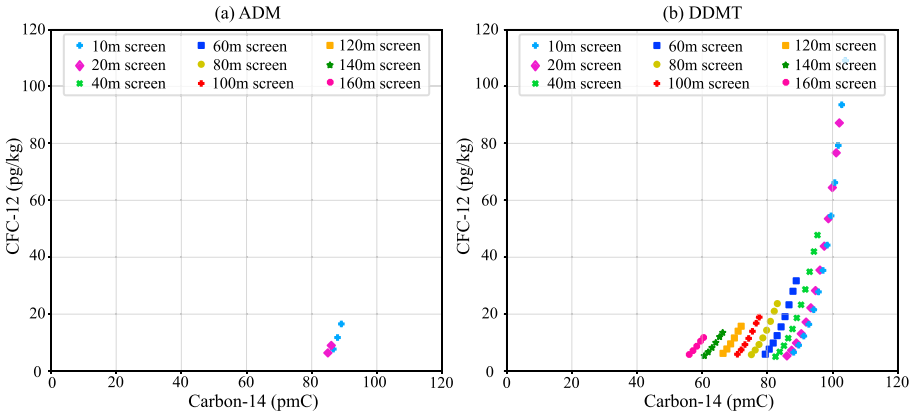

Figure 8. Comparison of reported model concentrations of CFC-12 and ^{14}C from all well screen iterations located at x = 1,550 m in the (a) advection macrodispersion model where θ = 0.2 and (b) dual-domain mass transfer model where θ_m = 0.01, θ_{im} = 0.19 and $\beta = 3.65 \times 10^{-6}$ year^{-1}. ADM = advection macrodispersion model; DDMT = dual-domain mass transfer.

located in the areas in which the most significant tracer biases were observed (x = 1,750 m for two recharge zones and x = 12,00 m for three recharge zones). These locations are positioned just short of what would be considered a *stagnant zone*, which in turn could be responsible for creating older water and a more complex pattern of mixing as water from different flow systems merge.

3.1.4. Scenario 4: Temporally Variable Recharge

The results of the transient recharge simulations suggest that the timing of the *wet* periods have the greatest significance on the present day environmental tracer concentrations, comparable to earlier findings from Schwartz et al. (2010). Period 2, which consists of extreme volume floods and correspondingly a higher recharge rate, causes a high rate of inflow of younger water into the deeper aquifer sections. The historic pattern of ^{14}C created by the low recharge period that represented the mega drought, whether this lasted for 1 or 10 kyr, is therefore replenished and nearly reset with a new distribution of young ^{14}C activities. Similarly, this period of higher recharge causes younger ^{39}Ar within the aquifer and fewer reported discrepancies in comparison to the steady state approximation (Figure 6e). If the drought period persisted for 10 kyr, then ^{14}C concentrations as low as 35 pmC could be recorded at the present day (Figure 5e). Despite these low concentrations, it is clear from the narrow shape of the output plots (Figures 5e and 6e) that the DDMT model, which assumes a temporally constant recharge and hence no significant wet period (Scenario 2), causes greater mixing of tracer concentrations than accounting for known historic recharge transients. The DDMT model effectively imposes mixing on the scale of the inverse of β. This could be because the model is only able to mix waters of ages corresponding to certain recharge periods rather than a continuous recharge input and the associated range of ages in the original DDMT model (Figures 5b and 6b). Interestingly, the temporally varying recharge results in the lowest ^{14}C activities with CFC-12 concentrations present. Therefore, while the envelope created by the temporally varying recharge has a lower vertical response, it does provide a mechanism for the contribution of old water to groundwater systems. It is clear from these simulations that for an accurate interpretation of old age-dating tracers such as ^{14}C, prior knowledge of flow transience within regional flow could be important, especially if significant wet or dry periods persisted.

3.1.5. Effect of Screen Length

A key output of this study was to determine what effect sampling conditions could have on reported field concentrations. It is well known that groundwater wells with long screens may sample a mixture of groundwater of different ages (Manning et al., 2005). While our results confirmed this for the DDMT simulations, with discrepancies being correlated with screen length, this was not the case for the ADM simulations. In the ADM simulations, no wells greater than 20 m in length reported detectible levels of both CFCs and ^{14}C (Figure 8). This is due to the fact that the small amounts of CFCs that were recharged under the assumed semiarid conditions were only sampled in the topmost sections of the screens. In longer screens the low concentrations were further diluted and thus falling below the detection limits. In contrast, the low porosities associated with the mobile domains represented in the DMMT model enable recharged CFC-12

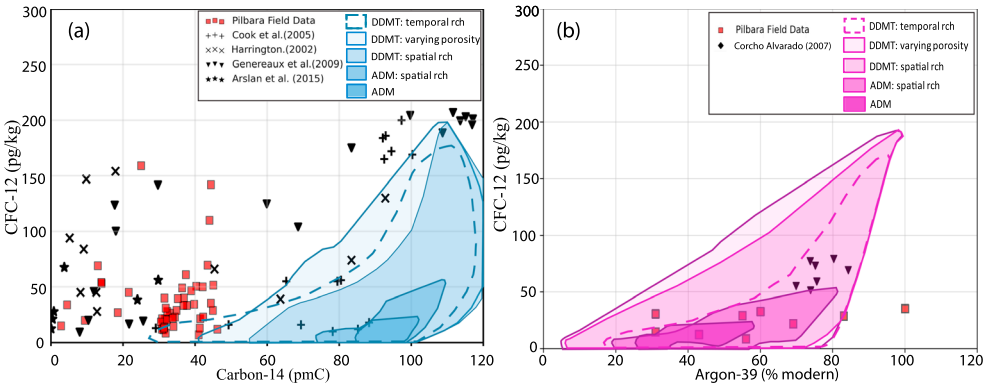

Figure 9. Comparison of samples collected in the Pilbara region and by other field studies with model concentrations from all well screen iterations located at x = 1,750 m for each scenario with a recharge rate of 5 mm/year. This figure represents the limit of mixing that can be obtained using purely physical mechanisms with each shade representing a different scenario by creating envelopes around the outermost points in each of the scenario plots in Figures 5 and 6. ADM = advection macrodispersion model; DDMT = dual-domain mass transfer.

to penetrate deeper into the aquifer. The widespread joint occurrence of old and young groundwater as reported, for example, in Jasechko et al. (2017) therefore implies that more complex transport and mixing mechanisms must occur in the corresponding aquifers.

3.2. Analysis of Pilbara Field Data

3.2.1. Relative Age Discrepancies

Figure 9 presents a comparison of the simulated concentrations generated for each model scenario with the raw field data collected from the Pilbara region and other previously reported field studies. Each envelope outlines the concentration distributions for each different scenario (as seen in Figures 5 and 6), and together they define the limits of discrepancies between tracers that might be generated by a particular physical process. The figure clearly illustrates that an ADM alone, considering no other processes, is unable to simulate a characteristic tracer behavior similar to that observed for the reported field sites, regardless of the monitoring bore screen length. In comparison to the ADM simulations, where the envelopes are very narrow, simulations incorporating DDMT produce a much larger envelope, indicating a greater mixing of disparate age tracer species is possible. What becomes apparent from Figure 9 is that with all simulations (except the standard ADM), the models can encapsulate the measured CFC-12 and ^{39}Ar data; however, the ^{14}C data cannot be matched with the physical processes considered. While a DDMT model has been successful at simulating tracer behavior in other studies, such as the highly heterogeneous Macrodispersion Experiment field site (Feehley et al., 2000; Harvey & Gorelick, 2000; Julian et al., 2001), our results suggest that physical mechanisms alone will not be able to generate the apparent age discrepancies reported for the field sites in our study.

3.2.2. Geochemical Reactions

When comparing the tracer samples collected from the Pilbara region and the results of the numerical experiments (Figure 9), it is evident that physical mechanisms alone are unable to generate the apparent ^{14}C-CFC age discrepancies that were reported. This finding suggests that additional processes are therefore necessary to shift the field data into the mixing envelopes. Such processes may include geochemical reactions such as carbonate weathering or the oxidation of organic carbon.

These processes lower the ^{14}C activity in aquifers and thus cause an overestimation of groundwater ages (Clark & Fritz, 1997; Cook et al., 2017; Han & Plummer, 2013; McCallum et al., 2017; Salmon et al., 2015). In the previous studies undertaken in the Pilbara region, Cook et al. (2017) corrected samples using the Pearson Model (Ingerson & Pearson, 1964), whereas McCallum et al. (2017) used the Mook Model (Han & Plummer, 2013). This in part reflects the large uncertainty associated with choosing the most appropriate ^{14}C correction scheme and parameters. For this study, both methods of radiocarbon correction were performed on the Pilbara ^{14}C field concentrations and compared. The Mook Model is a corrective model for open system carbonate dissolution that accounts for both carbonate dissolution caused by reaction

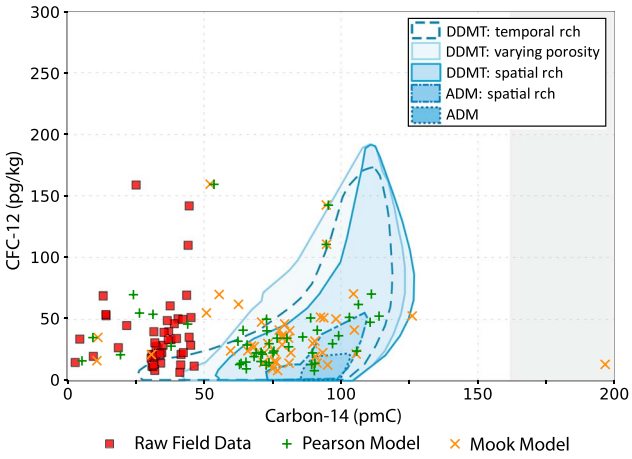

Figure 10. Comparison of CFC-12 versus Carbon-14 model simulation results with the Pilbara raw field data and the Pilbara data corrected using two different ^{14}C correction methods: the Mook model correction method and the Pearson model. Note that for the given parameters, both correction models have resulted in unrealistic corrections with values greater than the maximum possible decay-corrected ^{14}C activity (>160 pmC).
ADM = advection macrodispersion model; DDMT = dual-domain mass transfer.

with dissolved soil CO_2 and carbon exchange between dissolved inorganic carbon and gaseous CO_2 in the unsaturated zone (Mook, 1976, 1980). The Pearson's model is an alternative, widely applied model which accounts for a simple binary mixing process under closed-system conditions (Clark & Fritz, 1997; Ingerson & Pearson, 1964) and considers both the dissolved inorganic carbon activities of soil CO_2 and carbonate minerals. Based on recent field investigations, the end-member parameters were slightly adjusted from those chosen in the previous studies. An initial $\delta^{13}C$ value of −22‰ and a carbonate $\delta^{13}C$ from the Wittenoom Formation dolomite of 1‰, with a ^{14}C activity of 0 pmC (Becker & Clayton, 1972) was assumed. Figure 10 compares the raw ^{14}C field data and data corrected using both the Mook Model and Pearson method with the model simulation results for each scenario.

From Figure 10, it is apparent that both correction models immediately shift the raw field data into the mixing envelopes created by the model simulations. Sixty-eight percent of the field samples can be explained by the Mook Model correction in combination with mixing caused by a DDMT model. Similarly, 67% of samples can be explained by both the Pearson correction and DDMT. In comparison, only 19% and 10% of field samples could be explained by the ADM in combination with the Mook or Pearson model, respectively. Roughly 30% of samples remain unexplained by physical mixing in combination with geochemical processes. This could be because the correction methods or end member parameters selected were not the most appropriate for these individual field samples or that other reaction processes such as excess air are affecting the sample. It is clear from these results, however, that despite the corrections on the ^{14}C data, a DDMT mechnism is still required to create a tracer mixing envelope that encapsulates the field data. This suggests that this type of transport mechanism, as, for example, created by an extensive fracture network, is characterizing the flow and solute transport at the field site.

4. Conclusions

This study provides an improved understanding of the behavior of environmental tracers and their potential impact on groundwater age interpretations for a range of the most commonly considered physical transport phenomena and combinations of those phenomena. Previous studies have suggested that complexity in the physical settings can be more important than geochemical factors in interpreting groundwater age (Schwartz et al., 2010). The present study explicitly examined the effects of purely physical processes on concentrations of environmental tracers for a range of simple hydrogeological settings in combination with multiple monitoring well lengths.

Based on the results of our numerical experiments, we suggest that if large apparent age discrepancies between tracers of various temporal scales are recorded, it is unlikely that the solute transport at the respective site will be adequately represented by a standard ADM. Among the physical processes that were investigated in the present study, aquifer heterogeneity when represented through a DDMT model caused the most significant apparent age discrepancies. Models characterized by small mobile porosity values might be representative of highly fractured aquifer system, where younger groundwater can rapidly migrate over larger transport distances, while the immobile domain (matrix) contains relatively old groundwater. The mixing of these waters through interdomain mass transfer leads to the greatest simulated apparent age discrepancies. These findings, in combination with the widespread occurrence of mixtures between young and very old waters as recently reported by Jasechko et al. (2017), imply that dual-domain type solute transport phenomena affects environmental tracer transport behavior more significantly than previously thought.

Models incorporating matrix diffusion into immobile regions created a better fit to the CFC-12 and ^{39}Ar data from the Pilbara study site, though field data was limited. However, none of the investigated physical transport processes was able to explain the raw ^{14}C data. It is highly likely that geochemical or other

reaction processes could be affecting the field data, at least at the Pilbara field site. Once geochemical reaction processes were applied to the data, 68% of the field samples shifted to be within the mixing envelope.

Furthermore, the study also highlights the uncertainty over choosing the appropriate ^{14}C correction scheme if there is limited knowledge on the mineral source responsible for enrichment of $\delta^{13}C$. However, for this site both correction methods returned very similar results and created good fits over the tracer mixing envelopes. Even once the samples were corrected for ^{14}C reactions, the output concentrations still suggest that there is mixing of young and very old water. The corrections confirmed that ^{14}C corrections together with matrix diffusion processes results in the best fit to the field data. While roughly 30% of the samples can still not be explained when taking into account geochemical reactions, this could be because the most appropriate correction method or end member parameters were not selected or the use of unsuitable values to account for recharge temperature and excess air. More accurate determination of ^{14}C input activities, achieved using measurements of ^{14}C activities near the water table, could help improve the overall confidence in field scale models. This are particularly the case for the Mook Model, which is highly sensitive to end member parameters, pH and temperature. Regional flow models incorporating old tracers such as ^{14}C should also be tested in a transient setting to realistically account for marked changed in temporal patterns of recharge.

The addition of ^{39}Ar as an intermediate age tracer provides supporting evidence that the observed discrepancies are not caused by geochemical processes alone but must be a combined result with mixing processes, most likely due to matrix diffusion. This highlights the importance of using multiple environmental tracers of varying age ranges to calibrate groundwater flow models.

The numerical experiments presented here remain subject to several limitations. The intention of the study was not to present models as an exact representation of the field site, but rather as a tool to test a variety of hypotheses that explain the mixing of groundwater's of different ages. In doing so, we only considered a limited set of physical processes and combinations thereof. Also, the influence of transient pumping conditions on groundwater age discrepancies was also not closely investigated as it has been assessed in other studies (Engdahl, 2017; Zinn & Konikow, 2007a; Zuber et al., 2011). Nevertheless, the study provides a comprehensive assessment of field conditions that can lead to discrepant ages as reported by multiple environmental tracers and the limit to which physical processes alone can explain the often-observed discrepancies. Our modeling did not consider the effects of borehole integrity on groundwater ages. In long screen wells, ambient head gradients can water to migrate within the aquifer causing issues for age and environmental tracer analysis (Poulsen et al., 2018). With an increasing number of studies incorporating measured environmental tracer concentrations as calibration targets for solute transport models (e.g., Gusyev et al., 2013; Sonnenborg et al., 2016; Zuber et al., 2005), these findings will be useful to help resolve conceptual models of field sites when implementing numerical models.

Acknowledgments
This work was undertaken as part of a collaborative project between the National Centre for Groundwater Research and Training (NCGRT) and Rio Tinto Iron Ore. Funding was provided by the Australian Research Council and Rio Tinto Iron Ore. All data that were used in this study are provided in the supporting information.

References

Alikhani, J., Deinhart, A. L., Visser, A., Bibby, R. K., Purtschert, R., Moran, J. E., et al. (2016). Nitrate vulnerability projections from Bayesian inference of multiple groundwater age tracers. *Journal of Hydrology*, *543*, 167–181. https://doi.org/10.1016/j.jhydrol.2016.04.028

Amin, I. E., & Campana, M. E. (1996). A general lumped parameter model for the interpretation of tracer data and transit time calculation in hydrologic systems. *Journal of Hydrology*, *179*(1–4), 1–21. https://doi.org/10.1016/0022-1694(95)02880-3

Arslan, S., Yazicigil, H., Stute, M., Schlosser, P., & Smethie, W. M. (2015). Analysis of groundwater dynamics in the complex aquifer system of Kazan Trona, Turkey, using environmental tracers and noble gases. *Hydrogeology Journal*, *23*(1), 175–194. https://doi.org/10.1007/s10040-014-1188-z

Bauer, S., Fulda, C., & Schäfer, W. (2001). A multi-tracer study in a shallow aquifer using age dating tracers 3H, 85Kr, CFC-113 and SF6 — Indication for retarded transport of CFC-113. *Journal of Hydrology*, *248*(1–4), 14–34. https://doi.org/10.1016/S0022-1694(01)00381-X

Becker, R. H., & Clayton, R. N. (1972). Carbon isotopic evidence for the origin of a banded iron-formation in Western Australia. *Geochimica et Cosmochimica Acta*, *36*(5), 577–595. https://doi.org/10.1016/0016-7037(72)90077-4

Bedekar, V., Morway, E. D., Langevin, C. D., & Tonkin, M. J. (2016). MT3D-USGS version 1: A U.S. Geological Survey release of MT3DMS updated with new and expanded transport capabilities for use with MODFLOW, *Report Rep. 6-A53*, 84 pp, Reston, VA.

Bethke, C. M., & Johnson, T. M. (2008). Groundwater age and groundwater age dating. In *Annual review of Earth and planetary sciences* (pp. 121–152). Palo Alto: Annual Reviews.

Bretzler, A., Osenbruck, K., Gloaguen, R., Ruprecht, J. S., Kebede, S., & Stadler, S. (2011). Groundwater origin and flow dynamics in active rift systems - a multi-isotope approach in the Main Ethiopian rift. *Journal of Hydrology*, *402*(3–4), 274–289. https://doi.org/10.1016/j.jhydrol.2011.03.022

Busenberg, E., & Plummer, L. N. (1992). Use of chlorofluorocarbons (CCl3F and CFl2F2) as hydrologic tracers and age-dating tools—The alluvium and terrace system of Central Oklahoma. *Water Resources Research*, *28*, 2257–2283. https://doi.org/10.1029/92wr01263

Castro, M. C., & Goblet, P. (2005). Calculation of ground water ages--a comparative analysis. *Ground Water*, *43*(3), 368–380. https://doi.org/10.1111/j.1745-6584.2005.0046.x

Castro, M. C., Goblet, P., Ledoux, E., Violette, S., & de Marsily, G. (1998). Noble gases as natural tracers of water circulation in the Paris Basin 2. Calibration of a groundwater flow model using noble gas isotope data. *Water Resources Research*, *34*, 2467–2483. https://doi.org/10.1029/98wr01957

Clark, I. D., & Fritz, P. (1997). *Environmental isotopes in hydrogeology*. Boca Raton, Florida: Lewis Publishers.

Cook, P. G., & Böhlke, J.-K. (2000). Determining timescales for groundwater flow and solute transport. In P. G. Cook & A. L. Herczeg (Eds.), *Environmental tracers in subsurface hydrology* (pp. 1–30). Boston, MA: Springer US. https://doi.org/10.1007/978-1-4615-4557-6_1

Cook, P. G., Dogramaci, S., McCallum, J. L., & Hedley, J. (2017). Groundwater age, mixing and flow rates in the vicinity of large open pit mines, Pilbara region, northwestern Australia. *Hydrogeology Journal*, *25*(1), 39–53. https://doi.org/10.1007/s10040-016-1467-y

Cook, P. G., Hatton, T. J., Pidsley, D., Herczeg, A. L., Held, A., O'Grady, A., & Eamus, D. (1998). Water balance of a tropical woodland ecosystem, northern Australia: A combination of micro-meteorological, soil physical and groundwater chemical approaches. *Journal of Hydrology*, *210*(1–4), 161–177. https://doi.org/10.1016/S0022-1694(98)00181-4

Cook, P. G., & Herczeg, A. L. (2000). In P. G. Cook & A. L. Herczeg (Eds.), *Environmental tracers in subsurface hydrology*. Boston; London: Kluwer Academic.

Cook, P. G., Love, A. J., Robinson, N. I., & Simmons, C. T. (2005). Groundwater ages in fractured rock aquifers. *Journal of Hydrology*, *308*(1–4), 284–301. https://doi.org/10.1016/j.jhydrol.2004.11.005

Cook, P. G., & Robinson, N. I. (2002). Estimating groundwater recharge in fractured rock from environmental ^{3}H and ^{36}Cl, Clare Valley, South Australia. *Water Resources Research*, *38*(8), 1136. https://doi.org/10.1029/2001wr000772

Cook, P. G., & Solomon, D. K. (1995). Transport of atmospheric trace gases to the water-table—Implications for groundwater dating with chlorofluorocarbons and Krypton-85. *Water Resources Research*, *31*, 263–270. https://doi.org/10.1029/94wr02232

Corcho Alvarado, J. A., Purtschert, R., Barbecot, F., Chabault, C., Rueedi, J., Schneider, V., et al. (2007). Constraining the age distribution of highly mixed groundwater using ^{39}Ar: A multiple environmental tracer ($^{3}H/^{3}He$, ^{85}Kr, ^{39}Ar, and ^{14}C) study in the semiconfined Fontainebleau Sands Aquifer (France). *Water Resources Research*, *43*, W03427. https://doi.org/10.1029/2006WR005096

Cornaton, F., & Perrochet, P. (2006). Groundwater age, life expectancy and transit time distributions in advective-dispersive systems: 1. Generalized reservoir theory. *Advances in Water Resources*, *29*(9), 1267–1291. https://doi.org/10.1016/j.advwatres.2005.10.009

Cunnold, D. M., Fraser, P. J., Weiss, R. F., Prinn, R. G., Simmonds, P. G., Miller, B. R., et al. (1994). Global trends and annual releases of CCl_3F and CCl_2F_2 estimated from Ale/Gage and other measurements from July 1978 to June 1991. *Journal of Geophysical Research*, *99*, 1107–1126. https://doi.org/10.1029/93jd02715

D'Affonseca, F. M., Prommer, H., Finkel, M., Blum, P., & Grathwohl, P. (2011). Modeling the long-term and transient evolution of biogeochemical and isotopic signatures in coal tar–contaminated aquifers. *Water Resources Research*, *47*, W05518. https://doi.org/10.1029/2010WR009108

Dogramaci, S., Skrzypek, G., Dodson, W., & Grierson, P. F. (2012). Stable isotope and hydrochemical evolution of groundwater in the semi-arid Hamersley Basin of subtropical northwest Australia. *Journal of Hydrology*, *475*, 281–293. https://doi.org/10.1016/j.jhydrol.2012.10.004

Eberts, S. M., Bohlke, J. K., Kauffman, L. J., & Jurgens, B. C. (2012). Comparison of particle-tracking and lumped-parameter age-distribution models for evaluating vulnerability of production wells to contamination. *Hydrogeology Journal*, *20*(2), 263–282. https://doi.org/10.1007/s10040-011-0810-6

Ekwurzel, B., Schlosser, P., Smethie, W. M., Plummer, L. N., Busenberg, E., Michel, R. L., et al. (1994). Dating of shallow groundwater: Comparison of the transient tracers $^{3}H/^{3}He$, chlorofluorocarbons, and ^{85}Kr. *Water Resources Research*, *30*, 1693–1708. https://doi.org/10.1029/94WR00156

Engdahl, N. B. (2017). Transient effects on confined groundwater age distributions: Considering the necessity of time-dependent simulations. *Water Resources Research*, *53*, 7332–7348. https://doi.org/10.1002/2016WR019916

Feehley, C. E., Zheng, C. M., & Molz, F. J. (2000). A dual-domain mass transfer approach for modeling solute transport in heterogeneous aquifers: Application to the Macrodispersion Experiment (MADE) site. *Water Resources Research*, *36*, 2501–2515. https://doi.org/10.1029/2000wr900148

Freeze, R. A., & Cherry, J. A. (1979). *Groundwater* (p. 604). Englewood Cliffs, NJ: Prentice-Hall.

Fulton, S., Wohling, D., & Love, A. (2012). *Estimating recharge through an arid zone river; a comparison of groundwater tracer and physical techniques, Great Artesian Basin, Australia* (pp. 47–48). Boulder, CO: Geological Society of America (GSA).

Gardner, W. P., Hammond, G., & Lichtner, P. (2015). High performance simulation of environmental tracers in heterogeneous domains. *Ground Water*, *53*(S1), 71–80. https://doi.org/10.1111/gwat.12148

Gassiat, C., Gleeson, T., & Luijendijk, E. (2013). The location of old groundwater in hydrogeologic basins and layered aquifer systems. *Geophysical Research Letters*, *40*, 3042–3047. https://doi.org/10.1002/grl.50599

Gelhar, L. W., Welty, C., & Rehfeldt, K. R. (1992). A critical review of data on field-scale dispersion in aquifers. *Water Resources Research*, *28*, 1955–1974. https://doi.org/10.1029/92WR00607

Genereux, D. P., Webb, M., & Solomon, D. K. (2009). Chemical and isotopic signature of old groundwater and magmatic solutes in a Costa Rican rain forest: Evidence from carbon, helium, and chlorine. *Water Resources Research*, *45*, W08413. https://doi.org/10.1029/2008wr007630

Ginn, T. R. (1999). On the distribution of multicomponent mixtures over generalized exposure time in subsurface flow and reactive transport: Foundations, and formulations for groundwater age, chemical heterogeneity, and biodegradation. *Water Resources Research*, *35*, 1395–1407. https://doi.org/10.1029/1999wr900013

Goode, D. J. (1996). Direct simulation of groundwater age. *Water Resources Research*, *32*, 289–296. https://doi.org/10.1029/95wr03401

Gusyev, M. A., Toews, M., Morgenstern, U., Stewart, M., White, P., Daughney, C., & Hadfield, J. (2013). Calibration of a transient transport model to tritium data in streams and simulation of groundwater ages in the western Lake Taupo catchment, New Zealand. *Hydrology and Earth System Sciences*, *17*(3), 1217–1227. https://doi.org/10.5194/hess-17-1217-2013

Haggerty, R., & Gorelick, S. M. (1995). Multiple-rate mass-transfer for modeling diffusion and surface-reactions in media with pore-scale heterogeneity. *Water Resources Research*, *31*, 2383–2400. https://doi.org/10.1029/95wr01583

Han, L.-F., & Plummer, L. N. (2013). Revision of Fontes & Garnier's model for the initial ^{14}C content of dissolved inorganic carbon used in groundwater dating. *Chemical Geology*, *351*, 105–114. https://doi.org/10.1016/j.chemgeo.2013.05.011

Harrington, G. A. (2002). Recharge mechanisms to Quaternary sand aquifers in the Willunga Basin, *South Australia*.

Harvey, C. F., & Gorelick, S. M. (2000). Rate-limited mass transfer or macrodispersion: Which dominates plume evolution at the Macrodispersion Experiment (MADE) site? *Water Resources Research*, *36*, 637–650. https://doi.org/10.1029/1999wr900247

Hinsby, K., Hojberg, A. L., Engesgaard, P., Jensen, K. H., Larsen, F., Plummer, L. N., & Busenberg, E. (2007). Transport and degradation of chlorofluorocarbons (CFCs) in the pyritic Rabis Creek aquifer, Denmark. *Water Resources Research*, *43*, W10423. https://doi.org/10.1029/2006wr005854

Hofmann, T., Darsow, A., Groning, M., Aggarwal, P., & Suckow, A. (2010). Direct-push profiling of isotopic and hydrochemical vertical gradients. *Journal of Hydrology*, *385*(1–4), 84–94. https://doi.org/10.1016/j.jhydrol.2010.02.005

International Atomic Energy Agency (2006). Use of chlorofluorocarbons in hydrology: A guidebook, International Atomic Energy Agency, Vienna.

Ingerson, E., & Pearson, F. (1964). Estimation of age and rate of motion of groundwater by the 14C-method, *Recent researches in the fields of atmosphere, hydrosphere and nuclear geochemistry*, eds. Y. Miyake and T. Koyama, Marusen, Tokyo.263–283.

Jasechko, S., Perrone, D., Befus, K. M., Cardenas, M. B., Ferguson, G., Gleeson, T., et al. (2017). Global aquifers dominated by fossil groundwaters but wells vulnerable to modern contamination. *Nature Geoscience*, *10*(6), 425–429. https://doi.org/10.1038/Ngeo2943

Julian, H. E., Boggs, J. M., Zheng, C., & Feehley, C. E. (2001). Numerical simulation of a natural gradient tracer experiment for the natural attenuation study: Flow and physical transport. *Ground Water*, *39*(4), 534–545. https://doi.org/10.1111/j.1745-6584.2001.tb02342.x

Jurgens, B. C., Bexfield, L. M., & Eberts, S. M. (2014). A ternary age-mixing model to explain contaminant occurrence in a deep supply well. *Ground Water*, *52*(S1), 25–39. https://doi.org/10.1111/gwat.12170

Jurgens, B. C., Böhlke, J. K., Kauffman, L. J., Belitz, K., & Esser, B. K. (2016). A partial exponential lumped parameter model to evaluate groundwater age distributions and nitrate trends in long-screened wells. *Journal of Hydrology*, *543*, 109–126. https://doi.org/10.1016/j.jhydrol.2016.05.011

Kalin, R. M. (2000). Radiocarbon dating of groundwater systems. In P. G. Cook & A. L. Herczeg (Eds.), *Environmental tracers in subsurface hydrology* (pp. 111–144). Boston, MA: Springer US. https://doi.org/10.1007/978-1-4615-4557-6_4

LaBolle, E. M., Fogg, G. E., & Eweis, J. B. (2006). Diffusive fractionation of 3^H and ^{3}He in groundwater and its impact on groundwater age estimates. *Water Resources Research*, *42*, W07202. https://doi.org/10.1029/2005wr004756

Larocque, M., Cook, P. G., Haaken, K., & Simmons, C. T. (2009). Estimating flow using tracers and hydraulics in synthetic heterogeneous aquifers. *Ground Water*, *47*(6), 786–796. https://doi.org/10.1111/j.1745-6584.2009.00595.x

Leray, S., Engdahl, N. B., Massoudieh, A., Bresciani, E., & McCallum, J. (2016). Residence time distributions for hydrologic systems: Mechanistic foundations and steady-state analytical solutions. *Journal of Hydrology*, *543*, 67–87. https://doi.org/10.1016/j.jhydrol.2016.01.068

Levin, I., Bösinger, R., Bonani, G., Francey, R. J., Kromer, B., Münnich, K. O., et al. (1992). Radiocarbon in atmospheric carbon dioxide and methane: Global distribution and trends. In R. E. Taylor, A. Long, & R. S. Kra (Eds.), *Radiocarbon after four decades: An interdisciplinary perspective* (pp. 503–518). New York, NY: Springer. https://doi.org/10.1007/978-1-4757-4249-7_31

Liu, G. S., Zheng, C. M., & Gorelick, S. M. (2007). Evaluation of the applicability of the dual-domain mass transfer model in porous media containing connected high-conductivity channels. *Water Resources Research*, *43*, W12407. https://doi.org/10.1029/2007wr005965

Long, A. J., & Putnam, L. D. (2009). Age-distribution estimation for karst groundwater: Issues of parameterization and complexity in inverse modeling by convolution. *Journal of Hydrology*, *376*(3–4), 579–588. https://doi.org/10.1016/j.jhydrol.2009.07.064

Loosli, H., Möll, M., Oeschger, H., & Schotterer, U. (1986). Ten years low-level counting in the underground laboratoryin Bern, Switzerland. *Nuclear Instruments and Methods in Physics Research Section B: Beam Interactions with Materials and Atoms*, *17*(5–6), 402–405. https://doi.org/10.1016/0168-583X(86)90172-2

Loosli, H. H., Lehmann, B. E., & Smethie, W. M. (2000). Noble gas radioisotopes: ^{37}Ar, ^{85}Kr, ^{39}Ar, ^{81}Kr. In P. G. Cook & A. L. Herczeg (Eds.), *Environmental tracers in subsurface hydrology* (pp. 379–396). Boston, MA: Springer US. https://doi.org/10.1007/978-1-4615-4557-6_12

Loosli, H. H., & Purtschert, R. (2005). Rare gases. In P. K. Aggarwal, J. R. Gat, & K. F. O. Froehlich (Eds.), *Isotopes in the water cycle: Past, present and future of a developing science* (pp. 91–96). Dordrecht: Springer Netherlands. https://doi.org/10.1007/1-4020-3023-1_7

Ma, R., Liu, C., Greskowiak, J., Prommer, H., Zachara, J., & Zheng, C. (2014). Influence of calcite on uranium (VI) reactive transport in the groundwater–river mixing zone. *Journal of Contaminant Hydrology*, *156*, 27–37. https://doi.org/10.1016/j.jconhyd.2013.10.002

Maharajh, D. M., & Walkley, J. (1973). The temperature dependence of the diffusion coefficients of Ar, CO_2, CH_4, CH_3Cl, CH_3Br, and $CHCl_2F$ in water. *Canadian Journal of Chemistry*, *51*(6), 944–952. https://doi.org/10.1139/v73-140

Maloszewski, P., & Zuber, A. (1982). Determining the turnover time of groundwater systems with the aid of environmental tracers. 1. Models and their applicability. *Journal of Hydrology*, *57*(3–4), 207–231.

Małoszewski, P., & Zuber, A. (1982). Determining the turnover time of groundwater systems with the aid of environmental tracers. *Journal of Hydrology*, *57*(3–4), 207–231. https://doi.org/10.1016/0022-1694(82)90147-0

Małoszewski, P., & Zuber, A. (1985). On the theory of tracer experiments in fissured rocks with a porous matrix. *Journal of Hydrology*, *79*(3–4), 333–358. https://doi.org/10.1016/0022-1694(85)90064-2

Maloszewski, P., & Zuber, A. (1991). Influence of matrix diffusion and exchange-reactions on radiocarbon ages in fissured carbonate aquifers. *Water Resources Research*, *27*, 1937–1945. https://doi.org/10.1029/91wr01110

Maloszewski, P., & Zuber, A. (1996). *Lumped parameter models for the interpretation of environmental tracer data Rep*., 9–58 pp, IAEA, Vienna, Austria.

Manning, A. H., Kip Solomon, D., & Thiros, S. A. (2005). 3H/3He age data in assessing the susceptibility of wells to contamination. *Ground Water*, *43*(3), 353–367. https://doi.org/10.1111/j.1745-6584.2005.0028.x

Massoudieh, A., Visser, A., Sharifi, S., & Broers, H. P. (2014). A Bayesian modeling approach for estimation of a shape-free groundwater age distribution using multiple tracers. *Applied Geochemistry*, *50*, 252–264. https://doi.org/10.1016/j.apgeochem.2013.10.004

McCallum, J. L., Cook, P. G., Dogramaci, S., Purtschert, R., Simmons, C. T., & Burk, L. (2017). Identifying modern and historic recharge events from tracer-derived groundwater age distributions. *Water Resources Research*, *53*, 1039–1056. https://doi.org/10.1002/2016wr019839

McCallum, J. L., Cook, P. G., Simmons, C. T., & Werner, A. D. (2014). Bias of apparent tracer ages in heterogeneous environments. *Ground Water*, *52*(2), 239–250. https://doi.org/10.1111/gwat.12052

McGuire, K. J., McDonnell, J. J., Weiler, M., Kendall, C., McGlynn, B. L., Welker, J. M., & Seibert, J. (2005). The role of topography on catchment-scale water residence time. *Water Resources Research*, *41*, W05002. https://doi.org/10.1029/2004wr003657

Michael, H. A., & Voss, C. I. (2009). Controls on groundwater flow in the Bengal Basin of India and Bangladesh: Regional modeling analysis. *Hydrogeology Journal*, *17*(7), 1561–1577. https://doi.org/10.1007/s10040-008-0429-4

Mook, W. (1976). The dissolution-exchange model for dating groundwater with ^{14}C. In *Interpretation of environmental isotope and hydrochemical data in groundwater hydrology* (pp. 213–225). Vienna: IAEA.

Mook, W. (1980). Carbon-14 in hydrogeological studies. In *Handbook of environmental isotope geochemistry Vol. 1 The Terrestria Environment A* (pp. 49–74). Amsterdam: Elsevier.

Mook, W. G., Bommerson, J. C., & Staverman, W. H. (1974). Carbon isotope fractionation between dissolved bicarbonate and gaseous carbon dioxide. *Earth and Planetary Science Letters*, *22*(2), 169–176. https://doi.org/10.1016/0012-821x(74)90078-8

Neretnieks, I. (1980). Diffusion in the rock matrix: An important factor in radionuclide retardation? *Journal of Geophysical Research*, *85*, 4379–4397. https://doi.org/10.1029/JB085iB08p04379

Neretnieks, I. (1981). Age dating of groundwater in fissured rock—Influence of water volume in micropores. *Water Resources Research*, *17*, 421–422. https://doi.org/10.1029/WR017i002p00421

Neumann, R. B., Labolle, E. M., & Harvey, C. F. (2008). The effects of dual-domain mass transfer on the tritium-helium-3 dating method. *Environmental Science & Technology*, *42*(13), 4837–4843. https://doi.org/10.1021/es7025246

Niswonger, R. G., Panday, S., & Ibaraki, M. (2011). MODFLOW-NWT, A Newton formulation for MODFLOW-2005, Report Rep. *6-A37*.

Petersen, J., Deschamps, P., Gonçalvès, J., Hamelin, B., Michelot, J.-L., Guendouz, A., & Zouari, K. (2014). Quantifying paleorecharge in the Continental Intercalaire (CI) aquifer by a Monte-Carlo inversion approach of ^{36}Cl/Cl data. *Applied Geochemistry*, *50*, 209–221. https://doi.org/10.1016/j.apgeochem.2014.04.014

Poulsen, D. L., Cook, P. G., Simmons, C. T., McCallum, J. L., & Dogramaci, S. (2018). Effects of intraborehole flow on purging and sampling long-screened or open wells. *Groundwater*. https://doi.org/10.1111/gwat.12797

Purtschert, R., Yokochi, R., & Sturchio, N. (2013). Krypton-81 dating of old groundwater. In *International atomic energy agency, (ed.) Isotope methods for dating old groundwater* (pp. 319–324). Vienna: IAEA.

Reilly, T. E., Plummer, L. N., Phillips, P. J., & Busenberg, E. (1994). The use of simulation and multiple environmental tracers to quantify groundwater-flow in a shallow aquifer. *Water Resources Research*, *30*, 421–433. https://doi.org/10.1029/93wr02655

Riedmann, R. A., & Purtschert, R. (2016). Separation of argon from environmental samples for Ar-37 and Ar-39 analyses. *Separation and Purification Technology*, *170*, 217–223. https://doi.org/10.1016/j.seppur.2016.06.017

Rouillard, A., Skrzypek, G., Turney, C., Dogramaci, S., Hua, Q., Zawadzki, A., et al. (2016). Evidence for extreme floods in arid subtropical northwest Australia during the Little Ice Age chronozone (CE 1400-1850). *Quaternary Science Reviews*, *144*, 107–122. https://doi.org/10.1016/j.quascirev.2016.05.004

Salmon, S. U., Prommer, H., Park, J., Meredith, K. T., Turner, J. V., & McCallum, J. L. (2015). A general reactive transport modeling framework for simulating and interpreting groundwater14C age and δ13C. *Water Resources Research*, *51*, 359–376. https://doi.org/10.1002/2014wr015779

Samborska, K., Rozkowski, A., & Maloszewski, P. (2013). Estimation of groundwater residence time using environmental radioisotopes (14C,T) in carbonate aquifers, southern Poland. *Isotopes in Environmental and Health Studies*, *49*(1), 73–97. https://doi.org/10.1080/10256016.2012.677041

Sanford, W. E. (1997). Correcting for diffusion in carbon-14 dating of ground water. *Ground Water*, *35*(2), 357–361. https://doi.org/10.1111/j.1745-6584.1997.tb00093.x

Sanford, W. E. (2011). Calibration of models using groundwater age. *Hydrogeology Journal*, *19*(1), 13–16. https://doi.org/10.1007/s10040-010-0637-6

Sanford, W. E., Plummer, L. N., Casile, G., Busenberg, E., Nelms, D. L., & Schlosser, P. (2017). Using dual-domain advective-transport simulation to reconcile multiple-tracer ages and estimate dual-porosity transport parameters. *Water Resources Research*, *53*, 5002–5016. https://doi.org/10.1002/2016wr019469

Sanford, W. E., Plummer, L. N., McAda, D. P., Bexfield, L. M., & Anderholm, S. K. (2004). Hydrochemical tracers in the middle Rio Grande Basin, USA: 2. Calibration of a groundwater-flow model. *Hydrogeology Journal*, *12*(4), 389–407. https://doi.org/10.1007/s10040-004-0326-4

Sardin, M., Schweich, D., Leij, F. J., & Vangenuchten, M. T. (1991). Modeling the nonequilibrium transport of linearly interacting solutes in porous-media—A review. *Water Resources Research*, *27*, 2287–2307. https://doi.org/10.1029/91wr01034

Scanlon, B. R., Healy, R. W., & Cook, P. G. (2002). Choosing appropriate techniques for quantifying groundwater recharge. *Hydrogeology Journal*, *10*(1), 18–39. https://doi.org/10.1007/s10040-001-0176-2

Scanlon, B. R., Keese, K. E., Flint, A. L., Flint, L. E., Gaye, C. B., Edmunds, W. M., & Simmers, I. (2006). Global synthesis of groundwater recharge in semiarid and arid regions. *Hydrological Processes*, *20*(15), 3335–3370. https://doi.org/10.1002/hyp.6335

Schwartz, F. W., Sudicky, E. A., McLaren, R. G., Park, Y. J., Huber, M., & Apted, M. (2010). Ambiguous hydraulic heads and 14C activities in transient regional flow. *Ground Water*, *48*(3), 366–379. https://doi.org/10.1111/j.1745-6584.2009.00655.x

Siade, A., Nishikawa, T., & Martin, P. (2015). Natural recharge estimation and uncertainty analysis of an adjudicated groundwater basin using a regional-scale flow and subsidence model (Antelope Valley, California, USA). *Hydrogeology Journal*, *23*(6), 1267–1291. https://doi.org/10.1007/s10040-015-1281-y

Solomon, D. K., Genereux, D. P., Plummer, L. N., & Busenberg, E. (2010). Testing mixing models of old and young groundwater in a tropical lowland rain forest with environmental tracers. *Water Resources Research*, *46*, W04518. https://doi.org/10.1029/2009wr008341

Solomon, D. K., Schiff, S. L., Poreda, R. J., & Clarke, W. B. (1993). A validation of the ^{3}H/^{3}He method for determining groundwater recharge. *Water Resources Research*, *29*, 2951–2962. https://doi.org/10.1029/93WR00968

Solomon, D. K., & Sudicky, E. A. (1991). Tritium and helium 3 isotope ratios for direct estimation of spatial variations in groundwater recharge. *Water Resources Research*, *27*, 2309–2319. https://doi.org/10.1029/91WR01446

Sonnenborg, T. O., Scharling, P. B., Hinsby, K., Rasmussen, E. S., & Engesgaard, P. (2016). Aquifer vulnerability assessment based on sequence stratigraphic and ^{39}Ar transport modeling. *Groundwater*, *54*(2), 214–230. https://doi.org/10.1111/gwat.12345

Stauffer, F., Attinger, S., Zimmermann, S., & Kinzelbach, W. (2002). Uncertainty estimation of well catchments in heterogeneous aquifers. *Water Resources Research*, *38*(11), 1238. https://doi.org/10.1029/2001wr000819

Suckow, A. (2013). System analysis using multi-tracer approaches, in *Isotope methods for dating old groundwater*, Edited, pp. 217–244, IAEA, Vienna.

Sudicky, E. A., & Frind, E. O. (1981). Carbon 14 dating of groundwater in confined aquifers: Implications of aquitard diffusion. *Water Resources Research*, *17*, 1060–1064. https://doi.org/10.1029/WR017i004p01060

Sudicky, E. A., & Frind, E. O. (1982). Contaminant transport in fractured porous-media - analytical solutions for a system of parallel fractures. *Water Resources Research*, *18*, 1634–1642. https://doi.org/10.1029/WR018i006p01634

Sültenfuβ, J., Purtschert, R., & Führböter, J. F. (2010). Age structure and recharge conditions of a coastal aquifer (northern Germany) investigated with ^{39}Ar, ^{14}C, ^{3}H, He isotopes and Ne. *Hydrogeology Journal*, *19*(1), 221–236. https://doi.org/10.1007/s10040-010-0663-4

Talma, A. S., Weaver, J. M., Plummer, L. N., & Busenberg, E. (2000). In O. Sililo (Ed.), *CFC tracing of groundwater in fractured rock aided with ^{14}C and ^{3}H to identify water mixing*. Rotterdam: Balkema.

Toth, J. (1963). A theoretical analysis of groundwater flow in small drainage basins. *Journal of Geophysical Research*, *68*, 2354–2356. https://doi.org/10.1029/JZ068i008p02354

Troldborg, L., Refsgaard, J. C., Jensen, K. H., & Engesgaard, P. (2007). The importance of alternative conceptual models for simulation of concentrations in a multi-aquifer system. *Hydrogeology Journal*, *15*(5), 843–860. https://doi.org/10.1007/s10040-007-0192-y

Turnadge, C., & Smerdon, B. D. (2014). A review of methods for modelling environmental tracers in groundwater: Advantages of tracer concentration simulation. *Journal of Hydrology*, *519*, 3674–3689. https://doi.org/10.1016/j.jhydrol.2014.10.056

Varni, M., & Carrera, J. (1998). Simulation of groundwater age distributions. *Water Resources Research*, *34*, 3271–3281. https://doi.org/10.1029/98wr02536

Visser, A., Broers, H. P., Purtschert, R., Sültenfuß, J., & de Jonge, M. (2013). Groundwater age distributions at a public drinking water supply well field derived from multiple age tracers (^{85}Kr, ^{3}H/^{3}He, and ^{39}Ar). *Water Resources Research*, *49*, 7778–7796. https://doi.org/10.1002/2013WR014012

Vogel, J. (1967). Investigation of groundwater flow with radiocarbon, paper presented at isotopes in hydrology. Proceedings of a symposium.

Vogel, J. C., Thilo, L., & Vandijken, M. (1974). Determination of groundwater recharge with tritium. *Journal of Hydrology*, *23*(1–2), 131–140. https://doi.org/10.1016/0022-1694(74)90027-4

Wang, J. Z., Worman, A., Bresciani, E., Wan, L., Wang, X. S., & Jiang, X. W. (2016). On the use of late-time peaks of residence time distributions for the characterization of hierarchically nested groundwater flow systems. *Journal of Hydrology*, *543*, 47–58. https://doi.org/10.1016/j.jhydrol.2016.04.034

Warner, M. J., & Weiss, R. F. (1985). Solubilities of chlorofluorocarbon-11 and chlorofluorocarbon-12 in water and seawater. *Deep-Sea Research Part a-Oceanographic Research Papers*, *32*(12), 1485–1497. https://doi.org/10.1016/0198-0149(85)90099-8

Weissmann, G. S., Zhang, Y., LaBolle, E. M., & Fogg, G. E. (2002). Dispersion of groundwater age in an alluvial aquifer system. *Water Resources Research*, *38*(10), 1198. https://doi.org/10.1029/2001wr000907

Wilson, J. L., & Guan, H. (2004). Mountain-block hydrology and mountain-front recharge. In *Groundwater recharge in a desert environment: The southwestern United States* (pp. 113–137). Washington, DC: American Geophysical Union.

Wood, C., Cook, P. G., & Harrington, G. A. (2015). Vertical carbon-14 profiles for resolving spatial variability in recharge in arid environments. *Journal of Hydrology*, *520*, 134–142. https://doi.org/10.1016/j.jhydrol.2014.11.044

Wood, C., Cook, P. G., Harrington, G. A., & Knapton, A. (2017). Constraining spatial variability in recharge and discharge in an arid environment through modeling carbon-14 with improved boundary conditions. *Water Resources Research*, *53*, 142–157. https://doi.org/10.1002/2015wr018424

Yager, R. M., Plummer, L. N., Kauffman, L. J., Doctor, D. H., Nelms, D. L., & Schlosser, P. (2013). Comparison of age distributions estimated from environmental tracers by using binary-dilution and numerical models of fractured and folded karst: Shenandoah Valley of Virginia and West Virginia, USA. *Hydrogeology Journal*, *21*(6), 1193–1217. https://doi.org/10.1007/s10040-013-0997-9

Zhang, Y. C., Prommer, H., Broers, H. P., Slomp, C. P., Greskowiak, J., Van Der Grift, B., & Van Cappellen, P. (2013). Model-based integration and analysis of biogeochemical and isotopic dynamics in a nitrate-polluted pyritic aquifer. *Environmental Science and Technology*, *47*(18), 10,415–10,422.

Zheng, C. (2010). MT3DMS v5.3 supplemental user's guide *Rep*., Department of Geological Sciences, The University of Alabama, Tuscaloosa, Alabama

Zheng, C., & Wang, P. P. (1999). MT3DMS: A modular three-dimensional multispecies transport model for simulation of advection, dispersion, and chemical reactions of contaminants in groundwater systems; documentation and user's guide *Rep*., DTIC Document.

Zinn, B. A., & Konikow, L. F. (2007a). Potential effects of regional pumpage on groundwater age distribution. *Water Resources Research*, *43*, W06418. https://doi.org/10.1029/2006wr004865

Zinn, B. A., & Konikow, L. F. (2007b). Effects of intraborehole flow on groundwater age distribution. *Hydrogeology Journal*, *15*(4), 633–643. https://doi.org/10.1007/s10040-006-0139-8

Zuber, A. (1986). On the interpretation of tracer data in variable flow systems. *Journal of Hydrology*, *86*(1–2), 45–57. https://doi.org/10.1016/0022-1694(86)90005-3

Zuber, A., Różański, K., Kania, J., & Purtschert, R. (2011). On some methodological problems in the use of environmental tracers to estimate hydrogeologic parameters and to calibrate flow and transport models. *Hydrogeology Journal*, *19*(1), 53–69. https://doi.org/10.1007/s10040-010-0655-4

Zuber, A., Witczak, S., Różański, K., Śliwka, I., Opoka, M., Mochalski, P., et al. (2005). Groundwater dating with ^{3}H and SF_6 in relation to mixing patterns, transport modelling and hydrochemistry. *Hydrological Processes*, *19*(11), 2247–2275. https://doi.org/10.1002/hyp.5669